JCTC Journal of Chemical Theory and Computation

Article

pubs.acs.org/JCTC

Comprehensive Benchmark of Association (Free) Energies of Realistic Host−Guest Complexes

Rebecca Sure and Stefan Grimme*

Mulliken Center for Theoretical Chemistry, Institut für Physikalische und Theoretische Chemie, Universität Bonn Beringstr. 4, D-53115 Bonn, Germany

Supporting Information

ABSTRACT: The S12L test set for supramolecular Gibbs free energies of association ΔG_a (Grimme, S. *Chem. Eur. J.* **2012**, *18*, 9955−9964) is extended to 30 complexes (S30L), featuring more diverse interaction motifs, anions, and higher charges (−1 up to +4) as well as larger systems with up to 200 atoms. Various typical noncovalent interactions like hydrogen and halogen bonding, $\pi-\pi$ stacking, nonpolar dispersion, and CH−π and cation−dipolar interactions are represented by "real" complexes. The experimental Gibbs free energies of association (ΔG_a^{exp}) cover a wide range from −0.7 to −24.7 kcal mol^{-1}. In order to obtain a theoretical best estimate for ΔG_a, we test various dispersion corrected density functionals in combination with quadruple-ζ basis sets for calculating the association energies in the gas phase. Further, modern semiempirical methods are employed to obtain the thermostatistical corrections from energy to Gibbs free energy, and the COSMO-RS model with several parametrizations as well as the SMD model are used to include solvation contributions. We investigate the effect of including counterions for the charged systems (S30L-CI), which is found to overall improve the results. Our best method combination consists of PW6B95-D3 (for neutral and charged systems) or ωB97X-D3 (for systems with counterions) energies, HF-3c thermostatistical corrections, and Gibbs free energies of solvation obtained with the COSMO-RS 2012 parameters for nonpolar solvents and 2013-fine for water. This combination gives a mean absolute deviation for ΔG_a of only 2.4 kcal mol^{-1} (S30L) and 2.1 kcal mol^{-1} (S30L-CI), with a mean deviation of almost zero compared to experiment. Regarding the relative Gibbs free energies of association for the 13 pairs of complexes which share the same host, the correct trend in binding affinities could be reproduced except for two cases. The MAD compared to experiment amounts to 1.2 kcal mol^{-1}, and the MD is almost zero. The best-estimate theoretical corrections are used to back-correct the experimental ΔG_a values in order to get an empirical estimate for the "experimental", zero-point vibrational energy exclusive, gas phase binding energies. These are then utilized to benchmark the performance of various "low-cost" quantum chemical methods for noncovalent interactions in large systems. The performance of other common DFT methods as well as the use of semiempirical methods for structure optimizations is discussed.

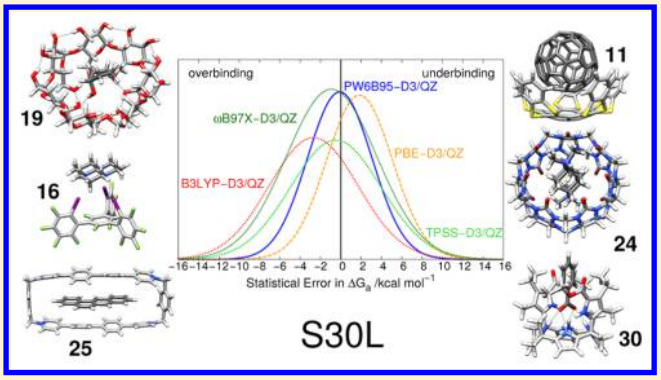

1. INTRODUCTION

Noncovalent interactions between atoms and molecules, such as dispersion interactions, $\pi-\pi$ stacking, or hydrogen and halogen bonding play an important role in structural biology and supramolecular chemistry.[1−3] They control the structures of DNA and proteins, antigen−antibody recognition, host−guest and enzyme−substrate binding, or the orientation of molecules on surfaces or in molecular crystals.[4,5] Because of their omnipresence in diverse fields of science, the investigation and understanding of these noncovalent interactions (NCIs) has advanced to a major topic in modern chemistry. Although they are frequently termed "weak" interactions, especially the London dispersion part can account for a large percentage of the total interaction energy and often outranks electrostatic or hydrogen bonding contributions.[6]

Noncovalently bound host−guest complexes are of particular importance in supramolecular chemistry. They are utilized in the fields of molecular recognition, template-direct synthesis, biomimetics, self-assembly, and even as reaction containers.[4,5,7−9] Therefore, the characterization and subsequent tuning of the different stabilizing interactions are of particular interest. Quantitative descriptions and predictions of the binding thermodynamics of these supramolecular complexes by means of computational electronic structure methods are still a challenge. This can be attributed to the fact that even the smallest experimentally synthesized systems are built up from a hundred atoms or more and that solvation and entropic effects play an important role in the binding process. Hence, the computational costs in a theoretical, preferably highly accurate quantum chemical treatment, are large and often unaffordable.

Received: March 30, 2015
Published: June 19, 2015

DOI: 10.1021/acs.jctc.5b00296
J. Chem. Theory Comput. 2015, 11, 3785−3801

Density functional theory (DFT) has been proven to provide a good ratio in terms of cost and accuracy for many applications in modern quantum chemistry. However, standard exchange-correlation functional approximations inherently lack the correct description of London (long-range) dispersion interactions.[10−12] Several different ways of treating dispersion forces within the Kohn−Sham DFT framework have been presented in the past years and have emerged as a standard in the field; for recent reviews, see refs 13 and 14, and for comparison of their performance, see, e.g., refs 15 and 16. As demonstrated recently, Gibbs free energies of association ΔG_a (in the following referred to as free energies) for typical medium-sized supramolecular host−guest systems can be computed with good accuracy by dispersion corrected density functional theory (e.g., DFT-D3[17]) together with a relatively large basis set in a nondynamic single-structure approach without any system-specific adjustments.[18−21] For the so-called S12L set of complexes,[18] which was the first benchmark set for NCIs in large systems, the DFT-D3 gas phase interaction energies were confirmed by independent DFT-SAPT calculations[22] and high level electronic Quantum Monte Carlo simulations.[23] For the related L7 benchmark set for NCIs in large model complexes, see ref 24.

Our procedure to obtain the target ΔG_a value involves three steps: First, the electronic interaction energy in the gas phase ΔE is computed for equilibrium structures. The molecules of interest (host, guest, and complex) are optimized in the gas phase on an affordable level including a dispersion correction, e.g., the TPSS meta-GGA density functional[25] together with the triple-ζ basis set def2-TZVP[26] and the D3 dispersion correction with Becke-Johnson damping[27,28] (D3(BJ)).[29] Single-point energies are obtained by employing a hybrid-functional like PW6B95[30]-D3 together with a large quadruple-ζ basis set, e.g., def2-QZVP.[26] The gas phase association energy ΔE is calculated in the supermolecular approach

$$\Delta E = E(\text{complex}) - E(\text{host}) - E(\text{guest}) \quad (1)$$

where E is the total electronic energy of the species involved. At a QZ basis set level, basis set superposition errors (BSSE) diminish to typically less than 2% of ΔE and can be ignored[19] for (hybrid)GGA functionals. In addition to the two-body dispersion interaction $\Delta E^{(2)}_{disp}$, the Axilrod−Teller−Muto-type three-body dispersion (ATM) energy $\Delta E^{(3)}_{disp}$ is also included. The three-body dispersion contribution to ΔE was found to be always positive and to contribute significantly with 2−3 kcal mol^{-1} for typical supramolecular systems.[18] We disregard many-body dispersion effects beyond the three-body term; see refs 23 and 31−34 for examples and further discussion. Note that $\Delta E^{(3)}_{disp}$ varies in methodologically different approaches,[23,35] and we decided to use the efficient D3 method for its computation without any empirical adjustments. However, missing higher-order many-body dispersion effects are maybe on the order of 1−2 kcal mol^{-1} which can be estimated from a comparison of D3+ATM data and the MBD approach[36] for molecular crystals.[37,38] This is relevant when aiming at absolute ΔG_a values of about 5−10 kcal mol^{-1}, and further investigation of their accurate computation seems mandatory. The total electronic interaction energy ΔE thus comprises the pure electronic DFT energy ΔE^{DFT}_{el}, two-body $\Delta E^{(2)}_{disp}$, and three-body dispersion energy $\Delta E^{(3)}_{disp}$:

$$\Delta E = \Delta E^{DFT}_{el} + \Delta E^{(2)}_{disp} + \Delta E^{(3)}_{disp} \quad (2)$$

Second, the sum of thermostatistical corrections from energy to free energy G^T_{RRHO} are obtained for each molecule in the gas phase at a given temperature T and normal pressure of 1 atm, including the zero-point vibrational energy. Since low-lying vibrational frequencies are inaccurate in the harmonic approximation, a modified rigid-rotor-harmonic-oscillator scheme is used.[18] In this approach, vibrational modes below 100 cm^{-1} are treated within a rigid-rotor model with smooth interpolation to the standard harmonic regime; for additional details, see ref 18. Its good performance has been verified repeatedly also for computing reaction thermochemistry; see, e.g., refs 39−41. The computation of the harmonic frequencies is carried out with semiempirical methods like PM6[42]-D3, DFTB[43]-D3 or our recently developed minimal basis set Hartree−Fock (HF-3c) method.[44] HF-3c is a fast quantum chemical procedure with three atom-pairwise correction terms (D3(BJ), geometrical counter-poise correction (gCP),[45] and an additional short-range term to correct for basis set deficiencies). It yields very reasonable structures and interaction energies for typical supramolecular systems and can therefore be used for preoptimizations or screening applications.

Third, a continuum solvation model like COSMO-RS[46,47] or SMD[48] is used in a black-box manner to calculate the solvation free energy $\delta G^T_{solv}(X)$ of each gas phase species at the temperature T in solvent X. The resulting values implicitly contain the conversion to standard state conditions. An alternative approach to the solvation problem is, for example, the coupling of quantum mechanics to an integral equation theory of liquids, like 3D-RISM.[49,50] As the current implementation unfortunately does not support all needed solvents, we did not apply this method here. Another route is represented by classical molecular dynamics (MD) or hybrid quantum mechanics/molecular mechanics (QM/MM) MD simulations, which require a statistical sampling of the distributions of solvent molecules; for recent examples, see refs 51 and 52.

The association free energy ΔG_a is the sum of the three contributions:

$$\Delta G_a = \Delta E + \Delta G^T_{RRHO} + \Delta\delta G^T_{solv}(X) \quad (3)$$

In the original publication,[18] this approach was applied to 12 rigid organic complexes (S12L) with up to 160 atoms and yielded accurate ΔG_a values with a mean absolute deviation (MAD) of only 2.1 kcal mol^{-1} with respect to the experiment for PW6B95-D3/def2-QZVP′ energies, DFTB-D3 vibrational frequencies, and solvation effects treated with COSMO-RS (2012 parametrization). Moreover, it has recently been employed in the SAMPL4 blind test challenge. Binding affinities for 14 cucurbit[7]uril complexes with cationic guest molecules were to be predicted, and our results ranked in the top three of all submissions in all statistical measures.[53−55]

The present work continues and extends the application of this approach to 30 complexes with up to 200 atoms and charges from −1 up to +4. In addition to 11 of the original complexes (excluding the ferrocene@CB7 complex because many semiempirical methods or force-fields cannot handle transition metals), 19 new chemically interesting complexes were chosen, which feature slightly less rigid hosts like crown ethers and cyclodextrins and host molecules with flexible alkyl side chains. The experimentally obtained ΔG_a values cover a wide range from −0.7 to −24.7 kcal mol^{-1}, and the complexes cover the most important typical supramolecular interactions such as hydrogen and halogen bonding, $\pi-\pi$ stacking, nonpolar

DOI: 10.1021/acs.jctc.5b00296
J. Chem. Theory Comput. 2015, 11, 3785−3801

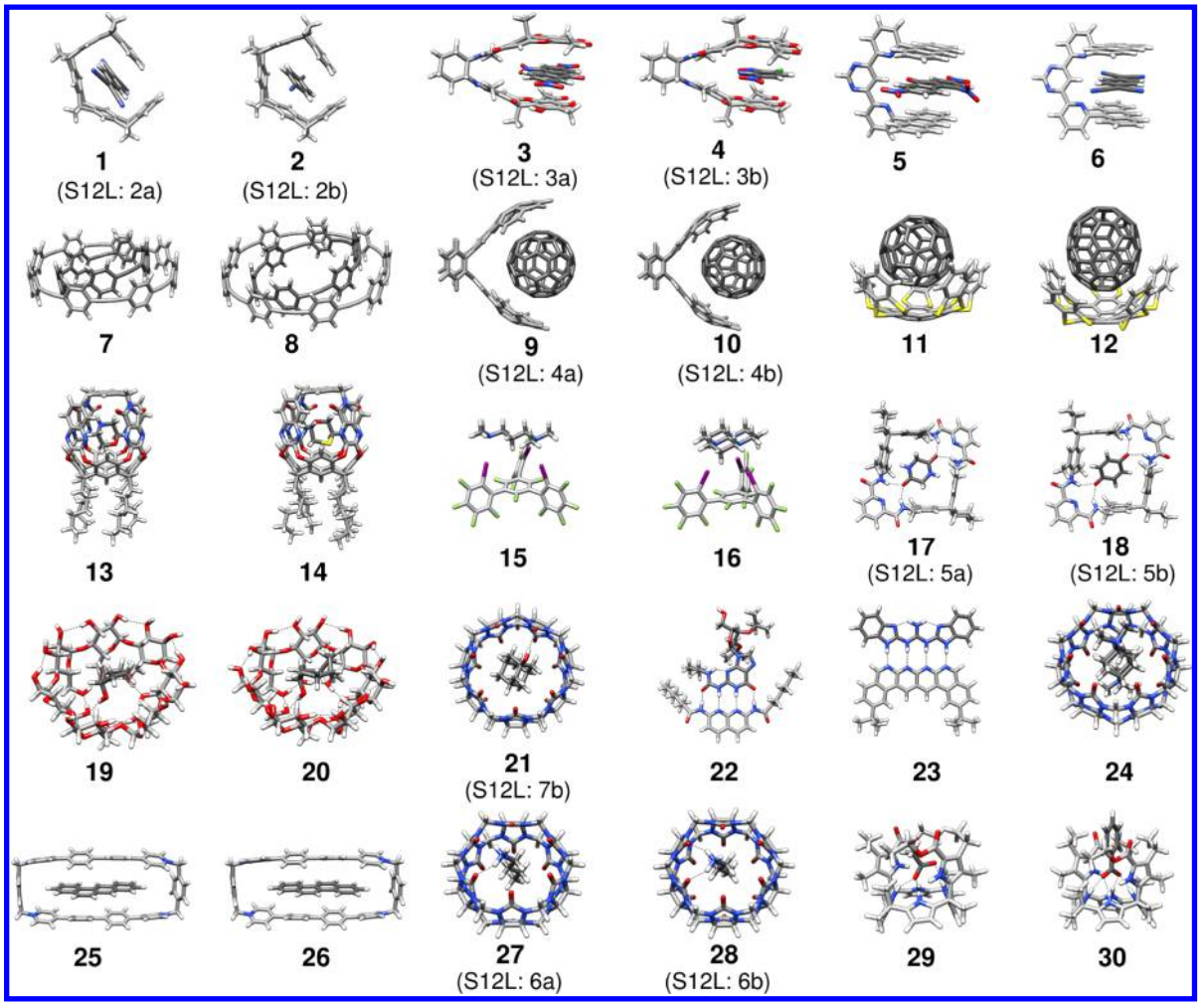

Figure 1. Structures of the 30 supramolecular complexes contained in the S30L test set. C atoms of the host molecules are shown in light gray, those of the guest molecules in dark gray, and H-bonding interactions are indicated by dotted lines. For convenience, the old S12L numbering is given if appropriate.

dispersion, CH−π, and cation−dipolar interactions. We investigate the influence of counterions for charged complexes since we found in previous studies that the inclusion of chloride (model) ions significantly improved the results.[20,54] Also, counterions were found to be necessary in calculations of multiply charged species when using the COSMO-RS solvation model.[56]

Furthermore, we test several density functionals to compute the binding energies, different semiempirical methods to calculate vibrational frequencies, and various COSMO-RS parametrizations as well as SMD to describe solvation effects in order to find the combination yielding the most accurate ΔG_a values. No empirical adjustments to any of the applied methods were made. With the presumably best approaches for ΔG^T_{RRHO} and $\Delta\delta G^T_{solv}$, we subsequently back-correct the experimental binding free energies to obtain empirical ("experimental") gas phase binding energies ΔE^{emp}. These values are then used to benchmark the performance of low-cost simplified quantum chemical methods and are suggested together with the best DFT values as reference data in future methodological studies.

1.1. Test Set Complexes. In the following, we briefly describe the investigated complexes. Figure 1 shows the optimized equilibrium structures of the complexes contained in the S30L test set, and Table 1 summarizes the experimental conditions as well as the net charges and the experimental ΔG_a^{exp} values. The complexes are sorted according to the most prominent type of interaction.

The first two complexes mainly feature nonpolar dispersion interactions and were already part of the S12L set. Compounds **1** and **2** are tweezer complexes with tetracyanoquinodimethane (TCNQ) and *para*-dicyanobenzene (DCB) (measured in $CHCl_3$ at 298 K).[57]

The next group consists of 10 complexes which mainly feature $\pi-\pi$ stacking interactions. Compounds **3** and **4** were taken from the S12L and are two pincer complexes with 2,4,7-trinitro-9-fluorenone (TNF) and 4-chloro-7-nitrobenzofurazan (NDB) as guests (in CH_2Cl_2 at 298 K).[58] Further, two tweezer complexes with TNF and TCNQ as guest molecules (**5** and **6** in $CHCl_3$ at 298 K)[59] were chosen. These two complexes are able to undergo shape switching and are therefore interesting as nanomechanical devices.[4,74] Also, two ring-in-ring complexes were considered, namely, [5]cycloparaphenyleneacetylene (5CPPA) in 8CPPA and 6CPPA in 9CPPA (**7** and **8** in $CHCl_3$ at 328 K).[60] These complexes show concave−convex $\pi-\pi$ interactions, which are important in the formation of, e.g., so-called bucky onions[75,76] and fullerene peapods.[77] Compound **7** has a ΔG_a value comparable to that of C_{60}@6CPPA

DOI: 10.1021/acs.jctc.5b00296
J. Chem. Theory Comput. 2015, 11, 3785−3801

Table 1. Overview of the Investigated Complexes, Their Charges (in the Case of S30L), the Experimental Measurement Conditions (Solvent and Temperature T in K), and the Experimental Association Free Energies ΔG_a^{exp} Given in kcal mol^{-1}

	complex	charge	solvent	T	ΔG_a^{exp}
1	TCNQ@tweezer[57]	0	$CHCl_3$	298	−4.2
2	DCB@tweezer[57]	0	$CHCl_3$	298	−1.4
3	TCNB@pincer[58]	0	CH_2Cl_2	298	−1.5
4	NBD@pincer[58]	0	CH_2Cl_2	298	−1.8
5	TNF@tweezer2[59]	0	$CHCl_3$	298	−5.2
6	TCNQ@tweezer2[59]	0	$CHCl_3$	298	−4.6
7	5CPPA@8CPPA[60]	0	$CHCl_3$	328	−5.5
8	6CPPA@9CPPA[60]	0	$CHCl_3$	328	−2.2
9	C_{60}@catcher[61]	0	toluene	293	−5.3
10	C_{70}@catcher[61]	0	toluene	293	−5.1
11	C_{60}@CA10[62]	0	CS_2	298	−4.4
12	C_{70}@CA10[62]	0	CS_2	298	−4.2
13	morpholine@RA4[63]	0	mesitylene	303	−10.0
14	tioxane@RA4[63]	0	mesitylene	303	−9.0
15	TMPDA@XB-donor[64]	0	cyclohexane	298	−0.7
15	HHTAP@XB-donor[64]	0	cyclohexane	298	−5.1
17	BQ@mcycle[65]	0	$CHCl_3$	298	−8.3
18	GLH@mcycle[65]	0	$CHCl_3$	298	−3.3
19	C_5H_9OH@β-CD[66]	0	H_2O	298	−3.0
20	$C_8H_{15}OH$@β-CD[66]	0	H_2O	298	−4.9
21	AdOH@CB7[67]	0	H_2O	298	−14.1
22	DAAD@ADDA[68]	0	$CHCl_3$	298	−11.7
23	AAAA@DDDD^{+}[69]	+1	CH_2Cl_2	298	−17.3
24	$Ad_2(NMe_3)_2$@CB7[70]	+2	H_2O	298	−24.7
25	tetraphene@Ex^2Box[71]	+4	CH_3CN	298	−4.4
26	chrysene@Ex^2Box[71]	+4	CH_3CN	298	−5.3
27	$BuNH_4^+$@CB6[72]	+1	formic acid/ H_2O 1:1	298	−6.9
28	$PrNH_4^+$@CB6[72]	+1	formic acid/ H_2O 1:1	298	−5.7
29	acetate@CP4[73]	−1	CH_3CN	298	−8.2
30	benzoate@CP4[73]	−1	CH_3CN	298	−7.7

giving evidence that concave−convex $\pi-\pi$ interactions are not limited to fullerenes only.[62,78] Compounds **9** and **10** were already part of the S12L and are two buckycatcher complexes that capture C_{60} and C_{70} (in toluene at 293 K).[61] Next, two other fullerene catcher complexes, pentakis(1,4-benzodithiino)-corannulene (CA10) as host and also C_{60} and C_{70} as guests (**11** and **12** in CS_2 at 298 K),[62] were chosen. In addition to the already mentioned concave−convex $\pi-\pi$ interactions, the CA10 host contains sulfur atoms, which provide somewhat enhanced dispersion interactions compared to those of second-row atoms.

The third group consists of two complexes which mainly show C−H···π interactions. Two resorcin[4]arene-based container (RA4) complexes with morpholine and tioxane as guests (**13** and **14** in mesitylene at 303 K) were selected.[63] These complexes feature nonpolar dispersion in addition to C−H···π interactions, and due to the latter, heterocyclic guests show a much larger binding affinity than cyclic hydrocarbons, which were also investigated experimentally. The RA4 container has four flexible hexyl side chains that were fully included in the calculations. Thus, **13** and **14** are the largest complexes with about 200 atoms.

The fourth group consists of two complexes which exhibit halogen bonding (**15** and **16** in cyclohexane at 298 K).[64] The host molecule (XB-donor) features three polyfluoroiodoarenes that are orientated perpendicular to the central benzene core and thus form a tridentate halogen bond donor motif. It binds various diamines and triamines such as the chosen guests *N*,*N*,*N*′,*N*′-tetramethylpropane-1,3-diamine (TMPDA) and hexahydro-1*H*,4*H*,7*H*-3*a*,6*a*,9*a*-triazaphenalene (HHTAP). Halogen bonds are more directional than hydrogen bonds, and thus, describing these multipoint interactions is much more challenging.[79−81]

The fifth group of eight complexes feature hydrogen bonds as the major type of interaction. The first two complexes are two amine macroycyle (mcycle) complexes with benzoquinone (BQ) and glycine anhydride (GLH) from the S12L (**17** and **18** in $CHCl_3$ at 298 K).[65] Note that the electronic structure of BQ is somewhat nontrivial in the sense that some quantum chemical codes produce a wrongly occupied orbital guess in the D_{2h} symmetry so that the SCF converges to an incorrect excited state. Next, two β-cyclodextrin (β-CD) complexes with cyclopentanol and cyclooctanol as guests (**19** and **20** in H_2O at 298 K) were investigated.[66] Cyclodextrins possess a hydrophobic central cavity and a hydrophilic outer surface and can therefore be used to improve the delivery for poorly soluble drugs.[82] Therefore, in addition to hydrogen bonds, nonpolar dispersion is also important. Compounds **21** and **24** are two cucurbit[7]uril (CB7) complexes with 1-hydroxyadamantane (AdOH) (taken from S12L)[67] and a double positively charged diamantane diammonium ($Ad_2(NMe_3)_2$)[69] as guests (in H_2O at 298 K). Compound **23** shows an especially high ΔG_a due to the perfect alignment of the guest along the axis of the host and hence maximal dispersion interaction of the diamantane core with the hydrophobic region of the inner circumference of the CB7 and seven ion−dipole interactions of the NMe_3^+ groups with each carbonyl of the ureidyl portal. Over the past decade, the cucurbit[*n*]uril (CB[*n*], *n* = 5,6,7,8) family of molecular containers has advanced to a major tool for studying molecular recognition in water.[83−85] Guest molecules with a rigid hydrophobic core, such as ferrocene[86] or adamantane,[68,87] in combination with cationic ammonium groups, have been found to yield very large binding affinities. Further, two quadruple hydrogen bond arrays were chosen. The first one is an ADDA-DAAD type array where both host and guest are a double donor (D) and a double acceptor (A) (**22** in $CHCl_3$ at 298 K).[68] The second one is an AAAA-DDDD$^+$ complex, where the host molecule is a quadruple acceptor and the guest a positively charged quadruple donor (**23** in CH_2Cl_2 at 298 K).[70] This array exhibits exceptional stability for such a small system even in hydrogen bond disrupting solvents.

The last group contains eight charged complexes (**23** and **24** also belong to this group). We investigated two complexes of the recently synthesized Ex^2Box^{4+} macrocycle with tetraphene and chrysene (**25** and **26** in CH_3CN at 298 K).[71] This macrocycle, composed of two biphenyl-bridged bipyridinium units and thus a charge of +4, has the unusual capability of binding π-electron rich as well as π-electron-poor guests, either two small molecules at the same time or one large guest like the chosen tetraphene and chrysene. In this case, the main interaction occurs through $\pi-\pi$-stacking. Compounds **27** and **28** were already included in the S12L and are two CB6 complexes with butylammonium ($BuNH_3$) and propylammonium ($PrNH_3$) guests (in a 1:1 mixture of formic acid and H_2O at 298 K).[72] The last complexes that were investigated are two calix[4]pyrrole (CP4) complexes that bind various mono

DOI: 10.1021/acs.jctc.5b00296
J. Chem. Theory Comput. 2015, 11, 3785−3801

anions. Our chosen guests are acetate and benzoate (**29** and **30** in CH_3CN at 298 K).[73] Anions are usually more challenging for DFT methods than cations due to the fact that the energy of the highest molecular orbital is often calculated to be positive leading to artifical charge-transfer.

2. COMPUTATIONAL DETAILS

The geometries of the S30L complexes **1**, **2**, **3**, **4**, **9**, **10**, **17**, **18**, **21**, **27**, and **28** as well as those of their host and guest molecules were taken from ref 18. Geometry optimizations of all other complexes, hosts, and guests (applying the appropriate charge of the molecules) were done on the same level, that is employing the density functional TPSS[25] together with the triple-ζ basis set def2-TZVP.[26] Hence, opposed to other large complex benchmarks like the L7 set,[24] treatment of S30L requires the computation of the so-called relaxation energy, i.e., the effect of full optimization of all fragments. In all DFT calculations except for M06-2X, the D3 dispersion correction[17] with Becke-Johnson (BJ) damping[27−29] was used. In the case of the S30L-CI set, chloride counterions were added to the cationic structures and sodium ions to the anionic structures of the charged complexes **23** to **30** at appropriate positions and reoptimized on the TPSS-D3/def2-TZVP level using the COSMO continuum solvation model.[88] No significant effect to the host−guest binding by the specific choice of the counterions is expected, and they should mainly compensate for the present charges and reduce the electrostatic contribution to ΔE and the COSMO-RS solvation free energies. This approach was successfully applied before.[56,89,90] Symmetric molecules were always treated in their respective point group (*vide infra*). Corrections for basis set superposition error (except for HF-3c which uses gCP) were not made.

Single-point calculations for the final gas phase interaction energies were conducted at the PW6B95[30]-D3, B3LYP[91−94]-D3, BLYP[92,95]-D3, PBE[96,97]-D3, TPSS-D3, and ωB97X-D3[98] levels together with the quadruple-ζ basis set def2-QZVP′ (QZ) with discarded g- and f-functions on the non-hydrogen and hydrogen atoms, respectively.[26] For such a large basis set, the basis set superposition error (BSSE) almost vanishes (remaining BSSE at this level is typically 1−2% of ΔE; see ref 19), and hence, no special treatment, e.g., such as a computationally demanding counter-poise correction, is required. Basis set extrapolation (TZ,QZ) of the energies for similar complexes yielded at maximum a change of about 0.5 kcal mol^{-1} for ΔE.[20] For iodine, the pseudopotentials from the Stuttgart/Cologne group were used.[99]

All DFT calculations were performed using the TURBOMOLE 6.4 program package,[100,101] except for the ωB97X-D3 single points, which were carried out with ORCA 3.0.1,[102,103] and the M06-2X[104] single-points, which were calculated with TURBOMOLE 6.6. The resolution-of-identity (RI) approximation for the Coulomb integrals[105] was applied in all cases using matching default auxiliary basis sets.[106] For the integration of the exchange-correlation contribution, the numerical quadrature grids *m4* (*m5* in case of M06-2X)[107] and grid 5 (final-grid 6) were employed in TURBOMOLE and ORCA, respectively. In the geometry optimizations as well as for the single-point energies, the default convergence criteria were used (10^{-7} E_h for energies and 10^{-5} E_h/Bohr for gradients). The three-body contribution to the dispersion energy were calculated using the `dftd3` program.[108] Computations of TPSS-D3 frequencies for comparison were carried out numerically and in parallel with SNF 2.2.1,[109] and the values were used unscaled.

The HF-3c[44] method was used for calculations of harmonic vibrational frequencies, geometry optimizations, and energies. The HF part was computed using TURBOMOLE 6.4 (with the same convergence criteria as those given above), and the 3c-terms to the energy and the nuclear gradients were calculated with our own freely available code.[108] For the optimizations of complexes with counterions, the COSMO model was used. Computations of the HF harmonic vibrational frequencies were performed analytically using the `aoforce` code of TURBOMOLE. The 3c-contributions to the Hessian are computed numerically by two-point finite differences of analytical gradients.[108] To determine G^T_{RRHO}, the HF-3c vibrational frequencies were scaled with a factor of 0.86. For the host molecules tweezer, CA10, and XB-donor and complex **23**, small imaginary frequencies of about < i50 cm^{-1} were obtained and inverted to the corresponding positive value in order to minimize the error resulting from missing low-lying modes.

SCC-DFTB3-D3 energies, geometries, and frequencies were computed with DFTB+[110] using the full third-order correction,[111] self-consistent charges (SCC), and the empirical damping for hydrogen-containing pair potentials[43,112,113] together with the most recent Slater−Koster files provided by the group of Elstner.[114] For simplicity the SCC-DFTB3-D3 method is referred to as DFTB-D3. The SCC tolerance was set to 10^{-7} E_h, and refitted D3 parameters determined recently[115] were used. For the geometry optimizations, the `statpt` code of TURBOMOLE 6.4 was used for executing the relaxation steps, and again, for the complexes with counterions the COSMO model was employed. The DFTB-D3 frequencies were used unscaled for calculating G^T_{RRHO}. For some complexes (**4**, **22**, **23**, **27**, and **28**), host (XB-donor and CB6), and guest molecules (5CPPA, 6CPPA, TMPDA, DAAD, and acetate), small imaginary frequencies of about < i50 cm^{-1} were obtained and therefore inverted. Imaginary frequencies larger than i100 cm^{-1} were observed for TCNB and TNF, disregarded, and not used in the calculation of G^T_{RRHO}.

PM6-D3,[42] PM6-D3H2,[116] and PM7[117] calculations were carried out with MOPAC 2012[118] but employing the TURBOMOLE modules for executing the geometry relaxation steps. As the parametrization of the hydrogen bonding corrections was done in combination with D3 employing zero damping (termed D3(0)), we used this scheme consistently for all PM6-D3 calculations. The same holds for DFT with the M06-2X functional where only D3(0) is appropriate. For the H+ corrections,[119] we used our own code, and the H4 corrections[120] were computed using the standalone code provided by the Hobza group. Vibrational frequencies for PM6-D3 were calculated numerically using MOPAC 2012. To obtain G^T_{RRHO}, the frequencies were used unscaled. For most host molecules and most complexes, imaginary frequencies were obtained, and again, those smaller than i50 cm^{-1} were inverted and larger ones disregarded.

OM2[121] energies were calculated with MNDO 2005.[122] The SCF convergence criterion was set to 10^{-6} eV. The dispersion contribution was calculated using the `dftd3` standalone code.

The COSMO-RS solvation model[46,47] was used as implemented in COSMOtherm[123] employing the 2012, 2013, and 2014 BP86/def-TZVP parametrization as well as 2013 and 2014 BP86/def2-TZVPD parameters (dubbed fine parametrizations in the following). To obtain the solvation free energies, the standard procedure with two single-point

DOI: 10.1021/acs.jctc.5b00296
J. Chem. Theory Comput. 2015, 11, 3785−3801

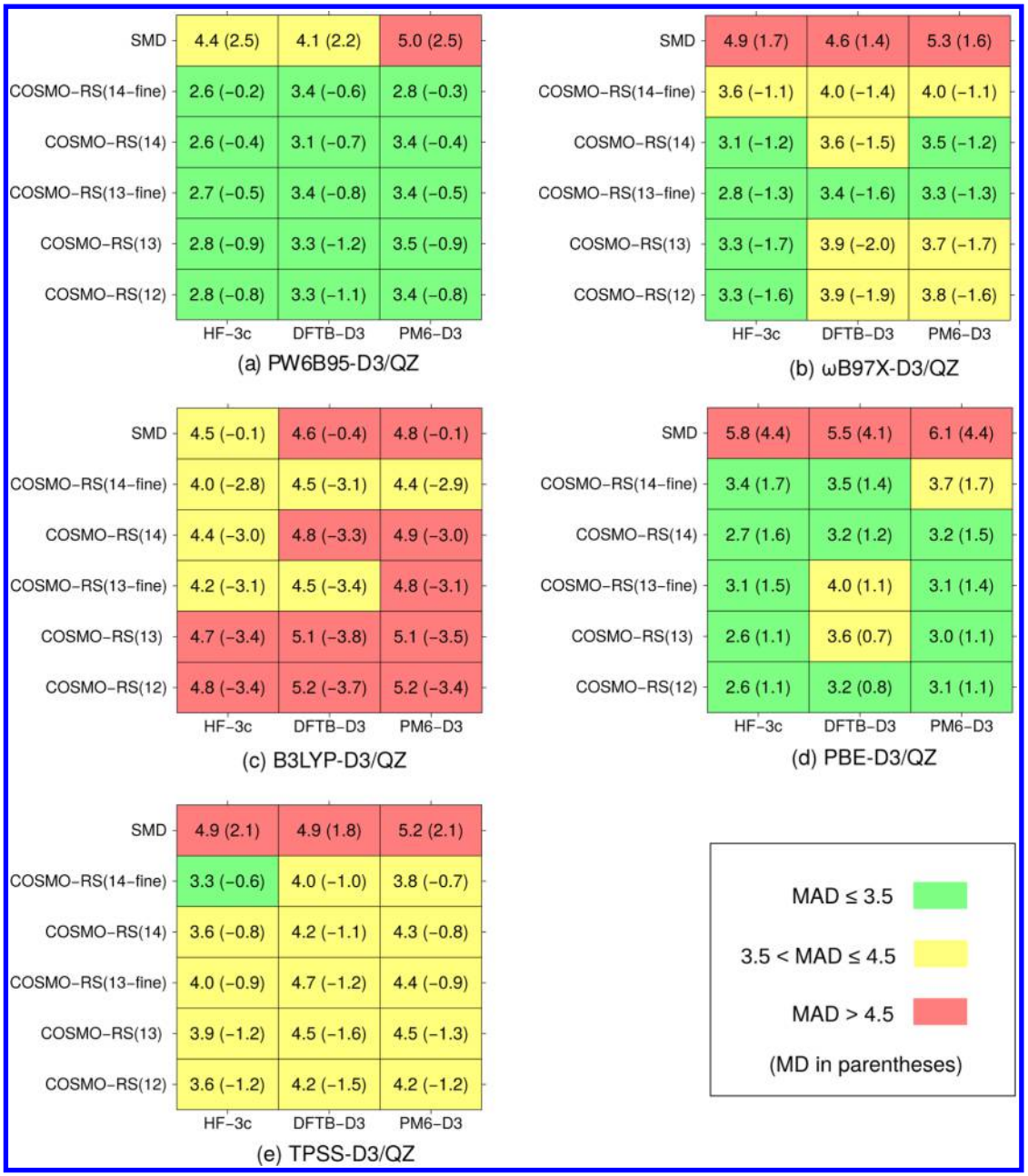

Figure 2. MADs (and MDs) for S30L for several combinations of functionals (ΔE), semiempirical methods for vibrational frequencies (ΔG^{T}_{RRHO}), and continuum solvation models ($\Delta\delta G^{T}_{solv}$) with respect to the experimental ΔG^{exp}_{a} values. A negative MD corresponds to overbinding and a positive one to underbinding. All values are given in kcal mol^{-1}.

calculations (one in the gas phase and one in an ideal conductor) on the default BP86[95,124]/def-TZVP[125] or BP86/def2-TZVPD[126] levels of theory were performed on the optimized gas-phase geometries and then used as input for COSMOtherm.

The SMD[48] calculations based on COSMO charges were performed on the BP86/def2-SVP level with the implementation in NWChem 6.4.[127] For the solvent mixture in the case of **27** and **28**, the solvation free energies were averaged.

All visualizations of molecules were done with USCF Chimera version 1.8.1,[128] and all graphs were plotted with Gnuplot 4.6.[129]

3. RESULTS AND DISCUSSION

Molecular symmetry influences the rotational part of the entropy, and the effect of the symmetry number σ is significant for highly symmetric molecules.[130] Therefore, we treated the symmetric guest and host molecules in their respective point group: C_{60} has I_h and C_{70} has D_{5h} symmetry; 5CPPA is D_{5h}, 6CPPA and CB6 D_{6h}, 8CPPA D_{8h}, and 9CPPA D_{9h} symmetric; TCNQ, DCB, TCNB, and BQ have D_{2h} symmetry; tetraphene has C_{2h} symmetry; benzoate and the tweezer are C_{2v} symmetric; XB-donor and HHTAP have C_{3v} symmetry; the pincer and tweezer2 are C_2 symmetric; FDNB, ADDA, crysene, acetate, CA10, DAAD, and AAAA are C_s symmetric; and $Ad_2(NMe_3)_2$ has C_i symmetry. Out of all complexes, only four exhibit any symmetry. Compound **9** is C_{2v}, **16** is C_{3v}, and **27** and **28** are C_s symmetric.

DOI: 10.1021/acs.jctc.5b00296
J. Chem. Theory Comput. 2015, 11, 3785−3801

The complexes **23**, **27**, and **28** are positively charged, **24** is doubly positively charged, **25** and **26** carry a 4-fold positive charge, and **29** and **30** are negatively charged. These systems were investigated with and without counterions. For simplicity, chloride ions were chosen for all cationic complexes and sodium ions for the anionic ones, although in the experiment iodide was present in the case of **24**, $[B(3,5\text{-}(CF_3)_2C_6H_3)_4]^-$ for **23**, and hexafluorophosphate in case of **25** and **26**. For an easier assignment of the systems, we will refer to the set without counterions as S30L and the one including them as S30L-CI. In general, we assume that the additional chloride or sodium ions do not effect the vibrations significantly. Hence, the same ΔG_{RRHO} values as those for the charged systems without counterions are used to calculate the final ΔG_a.

In the following sections, we evaluate the different possible method combinations for ΔG_a, investigate the influence of counterions, and find the presumably best method combination to reproduce the experimental values. With the help of the most accurate ΔG^T_{RRHO} and $\Delta G^T_{solv}(X)$, empirical ("experimental") binding energies are created and used for benchmarking low-cost semiempirical methods. Finally, the performance of these semiempirical methods for the geometries of the complexes is discussed.

3.1. Evaluating the Various Method Combinations. The three (free) energy components in eq 3 can independently be computed by different theoretical methods, and very many combinations are possible. A priori it is not clear if certain method combinations can benefit from error compensation and are thus preferred over others to compute accurate ΔG_a values. Finding such cases and exploring the general sensitivity of the results to the applied theory levels is the topic of this section. Note that it is currently not clear which of the three components ultimately limits the overall accuracy and in which direction future theoretical work should be invested.

For calculations of the binding energies, ΔE we tested the following functionals together with the D3(BJ) dispersion correction: PW6B95-D3 because it worked well for this purpose before[18,53] and yielded good results for the GMTKN30 general thermochemistry test set,[131] B3LYP-D3 and PBE-D3 because they are widely used, TPSS-D3 as another (meta-)GGA, and ωB97X-D3 as a long-range corrected range-separated hybrid which should be preferable for charged systems due to reduced self-interaction error. For all DFT calculations, the three-body dispersion (ATM) contribution is included, and D3(BJ)+ATM is abbreviated as just "D3" in the following, unless noted otherwise. The harmonic frequencies for the evaluation of ΔG^T_{RRHO} were calculated with the semiempirical methods HF-3c, PM6-D3, and DFTB-D3, and $\Delta G^T_{solv}(X)$ was obtained with COSMO-RS and SMD. For COSMO-RS, several parameter sets were used: the BP86/def-TZVP parameters from 2012, 2013, and 2014 and the BP86/def2-TZVPD parameters from 2013 and 2014 (called fine in the following).

Figure 2 shows the mean absolute deviation (MAD) from experiment (and the mean deviation (MD) in parentheses) for all possible method combinations. The values are color-coded in order to provide an easy overview as suggested by Martin and co-workers.[132]

The choice of the functional has the largest effect on the performance of the entire procedure. Within our of course limited test suite, PW6B95-D3 and PBE-D3 perform best yielding lowest MADs of about 3 kcal mol^{-1}. This confirms our previous finding that PW6B95-D3 yields accurate supramolecular binding energies. The good performance of PBE-D3 is somewhat surprising due to its known tendency to overbind hydrogen bonds.[38,131] However, we find that compared to, e.g., PW6B95-D3, the error for hydrogen bonded systems is here not larger than that for other complexes. ωB97X-D3 and TPSS-D3 give slightly worse results with MADs increased by about 0.5−1 kcal mol^{-1}. This conclusion is rather independent of the choice of the source of the thermostatistical as well as solvation corrections (see below). For B3LYP-D3, the MADs of about 5 kcal mol^{-1} are the largest obtained. The MD of B3LYP-D3 is also worst (about −3.5 kcal mol^{-1}) and indicates a strong tendency to overbind. This is also the reason why B3LYP-D3 is the only functional that does not yield worse results together with SMD as the SMD solvation contributions are usually larger than those from COSMO-RS. Since B3LYP-D3 performs very well for small noncovalently bound complexes,[133] we tentatively attribute this to an inconsistent treatment of many-body effects (see below) in this very over-repulsive functional (PW6B95, PBE, and TPSS are inherently much less repulsive).

The conclusion for the performance of the functionals is not affected by the inclusion of the three-body dispersion term. Disregarding it worsens almost all MADs by at least 0.5 kcal mol^{-1} when COSMO-RS is used as a solvation model. When SMD is employed, in most cases the MAD is better without the three-body dispersion due to the already mentioned larger values for $\Delta\delta G^T_{solv}$. For analysis purposes, we tested if scaling the three-body dispersion (in a range from 0.5 to 2.1) improves the performance. In the case of PW6B95-D3 and ωB97X-D3, the unscaled three-body contribution yields mean absolute deviations and standard deviations (SD) very close to the optimum. For PBE-D3, a slight improvement in both measures is observed when the three-body dispersion is scaled down; for TPSS-D3, a slight improvement is gained when it is scaled up. In the case of B3LYP-D3, scaling up the three-body term yields a significant improvement of 0.5 kcal mol^{-1} of both the MAD and SD. This is consistent with the finding that B3LYP-D3 shows a strong tendency to overbind. TPSS-D3 and B3LYP-D3 both have a relatively large scaling factor s_8 of about two for the higher order two-body dispersion term in the D3 scheme. To check whether this might be connected, we also tested the BLYP functional, which has a similarly large s_8 value of about 2.7. The behavior is the same as seen for B3LYP, and it is even more pronounced. Particularly, the complexes **9**−**12** with C_{60} or C_{70} as guests where the ATM term is large are overbound with these functionals. These observations suggest that functionals with a smaller s_8 value in the D3 scheme yield in general better results for the binding energies of large systems.

When comparing the semiempirical methods tested for the frequencies, it is evident that HF-3c performs slightly better than DFTB-D3, and both yield better results than PM6-D3. HF-3c also seems to be generally more stable for this purpose since HF avoids any quadrature schemes and is practically free of numerical noise. This is of particular importance for low-lying vibrational modes. Contrary to HF-3c, imaginary modes were obtained for a few complexes, host and guest molecules when DFTB-D3 was used (see Computational Details) and for almost all complexes when PM6-D3 was employed. For eight complexes (**1**, **3**, **7**, **9**, **15**, **17**, **22**, and **25**), we also calculated (unscaled) TPSS-D3/def2-TZVP vibrational frequencies to obtain ΔG^T_{RRHO} values for comparison. The HF-3c results agree very well with the DFT ones, and the absolute deviation is only 0.4 kcal mol^{-1} on average for the ΔG^T_{RRHO} term (see Supporting

DOI: 10.1021/acs.jctc.5b00296
J. Chem. Theory Comput. 2015, 11, 3785−3801

Information for details, Table S5). If PM6-D3 and DFTB-D3 used for the frequencies the MAD is larger, 1.1 and 1.6 kcal mol^{-1}, respectively. Note that anharmonic vibrational treatments for systems as large as the complexes discussed here are currently not possible.

For the solvation models, the trend is not as clear as for the functionals and the thermostatistical contributions. In general, COSMO-RS outperforms SMD, but several parametrizations yield equally good results. It has been reported before that SMD performs worse for ions than other SMx methods, e.g., SM6 or SM8.[134] Excluding the charged systems (**23** to **30**) improves the results for both solvation models slightly (see Supporting Information, Figure S1). As the improvement is similar, the charged complexes cannot cause the worse performance of SMD compared to that of the COSMO-RS. When COSMO-RS is used, the resulting MADs lie between 2.6 and 2.8 kcal mol^{-1} in combination with PW6B95-D3 energies and HF-3c thermostatistical corrections, and between 2.6 and 3.4 kcal mol^{-1} for PBE-D3 and ΔG^{T}_{RRHO}(HF-3c). We expected the 2014-fine parametrization to perform better than others because it uses the theoretically superior D3 scheme to describe solvation dispersion interactions instead of a much simpler surface-proportional approach employed for the other parameter sets, but this seems not to be the case. All COSMO-RS versions yield similar MADs and MDs, and for all of them, outliers are observed. This will be discussed in more detail in the next sections.

Overall, there is no method combination that very clearly outperforms others, and at this point, we recommend using the PW6B95-D3 functional (together with a quadruple-ζ basis set) for the gas phase association energies ΔE, HF-3c for the thermostatistical corrections ΔG^{T}_{RRHO}, and COSMO-RS for the solvation contributions $\Delta\delta G^{T}_{solv}$.

3.2. Influence of Counterions. The results discussed so far were obtained without including counterions for the charged systems **23** to **30**. In the S30L-CI test, chloride ions were included for the cationic systems and sodium ions for the anionic ones meaning that in all quantum chemical calculations of energeis (including those required by the continuum solvation models) only overall neutral species appear. The structures of complexes **23-CI** to **30-CI** are shown in Figure 3. As mentioned before, the same thermostatistical corrections as for the S30L were used, so they will not be discussed again.

Figure 4 shows the color-coded MADs with respect to experiment (and the MDs in parentheses) for all possible method combinations for the S30L-CI in the same manner as before. Whether the inclusion of counterions improves or deteriorates the results strongly depends on the functional. The largest improvement is observed for ωB97X-D3, which now outperforms PW6B95-D3. B3LYP-D3 also yields better results and now performs similar to TPSS-D3. For PW6B95-D3, the MADs stay similar, and for TPSS-D3 and PBE-D3, a slight deterioration is obtained compared to the results for S30L. The observations for the solvation contributions are the same as for S30L: COSMO-RS outperforms SMD for $\Delta\delta G^{T}_{solv}$, but the five versions give similar results.

The individual errors in ΔG_a for the charged complexes with respect to experimental data are shown for ωB97X-D3 in Figure 5. The largest improvement is observed for complex **24**. Without counterions, it is overbound by −11.1 kcal mol^{-1}, and upon inclusion of chloride ions, the error is reduced to only −0.3 kcal mol^{-1}. In the case of **23**, **25**, **26**, **27**, and **28**, the deviation compared to experiment decreases by about 2−4 kcal mol^{-1}. For **25** and **26**, the complexes with the highest charge of +4, the improvement is not larger when counterions are added than that for other complexes. Because of the fully conjugated π-system, the charges are highly delocalized and thus seem to cause less problems for the continuum solvation models compared to the more localized charges in the other systems. Other COSMO-RS parametrizations gave similar results in combination with the ωB97X-D3 functional for the six cationic systems. For other functionals, the improvement or deterioration upon inclusion of chloride ions can differ from the results shown for ωB97X-D3.

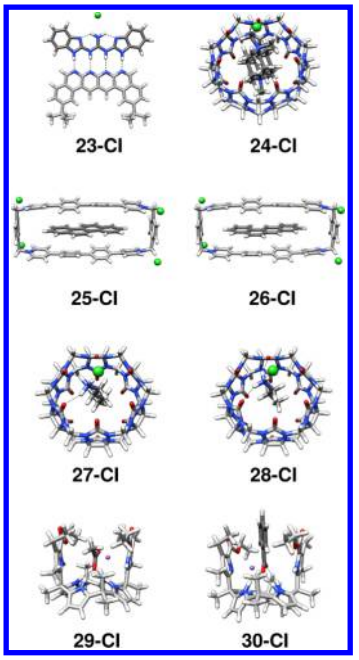

Figure 3. Structures of the eight supramolecular complexes contained in the S30L-CI test set which have counterions (chloride ions drawn in green, and sodium ions are purple). C atoms of the host molecules are shown in light gray, those of the guest molecules in dark gray, and H-bonding interactions are indicated by dotted lines.

In contrast, for the two anionic systems ωB97X-D3 yields worse results when sodium counterions are taken into account. All other functionals behave in the same way, though the extent of deterioration may differ. Again, these observations do not depend on the COSMO-RS parametrization employed. This result is surprising because the tested density functional approximations should have more problems in describing anions than cations, and this might suggest the general omission of sodium counterions for anionic systems.

3.3. Finding the Optimal Method Combination. As described above, PW6B95-D3 yields the best gas phase interaction energies for S30L, and ωB97X-D3 performs best for the S30L-CI set. HF-3c consistently gives the best thermostatistical contributions. In terms of MAD and MD, all COSMO-RS parametrizations perform similar, and for all of them, outliers exist.

Figure 6 (top) shows the comparison of the calculated ΔG_a with the experimental ΔG^{exp}_a for the S30L set when the COSMO-RS(12) parameters are used. For nonpolar solvents, like chloroform or dichloromethane, COSMO-RS(12) gives the most consistent results, which cannot be improved when any other parametrization is used. Compound **22** clearly is an outlier for all COSMO-RS versions. According to our previous experience, COSMO-RS(14-fine) yields better values for

DOI: 10.1021/acs.jctc.5b00296
J. Chem. Theory Comput. 2015, 11, 3785−3801

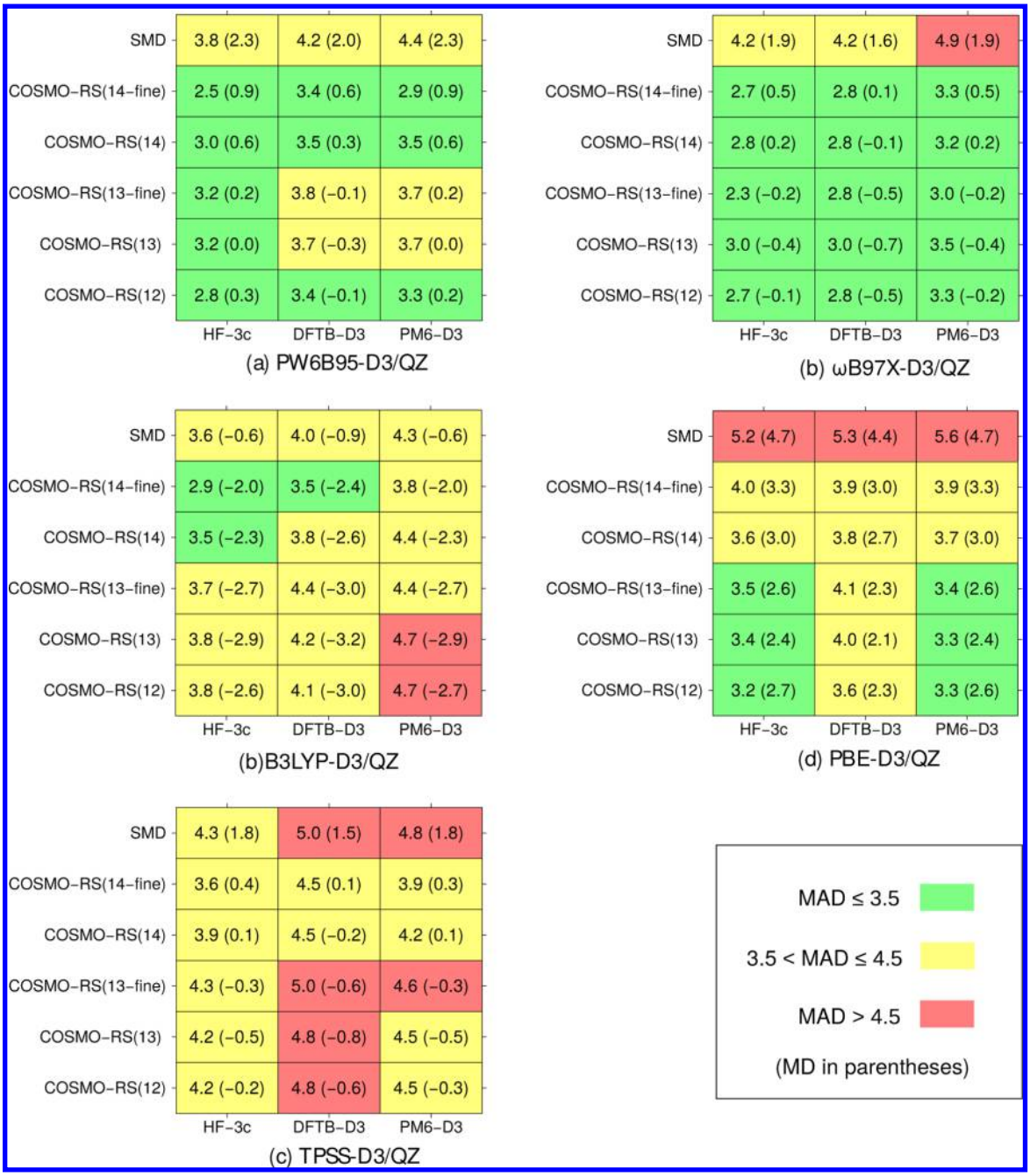

Figure 4. MADs (and MDs) for S30L-CI for several combinations of functionals (ΔE), semiempirical methods for vibrational frequencies (ΔG^{T}_{RRHO}), and continuum solvation models ($\Delta\delta G^{T}_{solv}$) with respect to the experimental ΔG^{exp}_{a} values. The three-body dispersion contribution $\Delta E^{(3)}_{disp}$ is always included. A negative MD corresponds to overbinding and a positive one to underbinding. All values are given in kcal mol^{-1}.

solvents like toluene, which can do $\pi-\pi$-stacking, in combinations with fullerene complexes due to the aforementioned better description of dispersion in COSMO-RS(14-fine).[20] For the two buckycatcher complexes **9** and **10** in toluene, the deviation of COSMO-RS(12) and COSMO-RS(14-fine) is small (up to 2 kcal mol^{-1}). Therefore, we decided to use the COSMO-RS(12) values. Moreover, the calculations are less time-consuming when the regular instead of the fine parametrizations are used.

For water as the solvent, the situation is different. With COSMO-RS(12), the complexes **21**, **24**, **27**, and **28** show a large deviation from experiment, which can be reduced when a fine parametrization is used. For the six complexes in water, the best and most consistent results were obtained with COSMO-RS(13-fine) (Figure 6 (bottom)). An explanation for this may be that the fine parametrizations employ the larger basis set def2-TZVPD instead of def-TZVP. It is well-known that for water a large basis set with diffuse functions is necessary for an accurate description.[131] The largest errors (≥4 kcal mol^{-1}) for S30L are now observed for **6**, **11**, **13**, **22**, **25**, and **26**. Complexes **6**, **11**, **25**, and **26** are overbound by −4.0, −5.4, −4.5, and 4.6 kcal mol^{-1}, respectively, while **13** and **22** are underbound by 4.9, and 8.9 kcal mol^{-1}, respectively.

Complex **11** belongs to the ones which have a fullerene as guest molecule. For these types of large, electronically delocalized systems, a partial breakdown of pairwise dispersion

DOI: 10.1021/acs.jctc.5b00296
J. Chem. Theory Comput. 2015, 11, 3785−3801

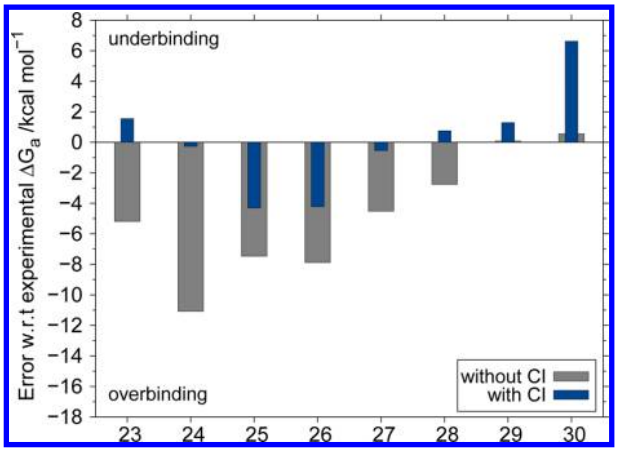

Figure 5. Deviations for the method combination ωB97X-D3/QZ, HF-3c, and COSMO-RS(13-fine) including and disregarding counterions for the charged systems **23** to **30** with respect to the experimental ΔG_a^{exp} in kcal mol^{-1}.

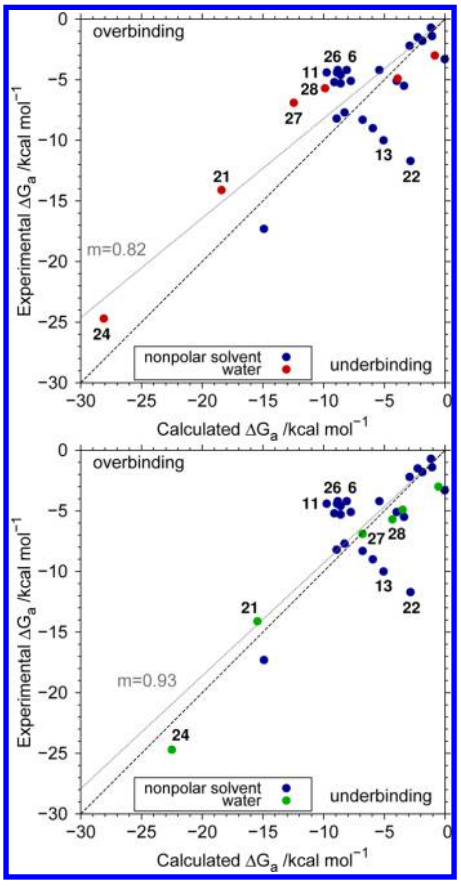

Figure 6. Comparison of experimental ΔG_a^{exp} and computed total free association energies ΔG_a for S30L obtained with the method combination PW6B95-D3/HF-3c/COSMO-RS(12) throughout (top), and PW6B95-D3/HF-3c/COSMO-RS(12) for nonpolar solvents, and COSMO-RS(13-fine) for water (bottom). The dashed gray line shows the result of a linear regression with slope *m*.

interaction schemes has been observed and analyzed before.[135,136] This is confirmed by our study as reflected in the overbinding observed for all complexes including fullerenes, though less pronounced for **9**, **10**, and **12**. Although within our D3 dispersion, model three-body-effects are only very approximately included, and the three-body dispersion for these four systems is qualitative correctly and found to be larger (3.3 to 5.1 kcal mol^{-1}) compared to that of other complexes (excluding **24**). Many-body-dispersion effects beyond the three-body term are disregarded in our model, but the observed overbinding provides evidence that neglecting the higher order terms introduces an error of about 1−2 kcal mol^{-1} for theses systems. Recent work on molecular crystals and comparison of D3 and MBD data indicate[37,38] that many-body effects beyond three-body dispersion are probably rather small for saturated or not too unsaturated organic molecules. This conclusion is in agreement with previous results from wave function theory based analysis (for cooperativity in noncovalent interactions of biologically relevant molecules, see ref 137, and for a study on crystalline benzene, see ref 33). For six of the complexes (**1**, **2**, **9**, **17**, **21**, and **27**), PBE-MBD* calculations exist.[23] Compared to our PBE-D3 values, the PBE-MBD* results for ΔE are always more negative, and the deviations lie in the range of −0.6 to −1.8 kcal mol^{-1} for five of the complexes. For **21**, the deviation is −4 kcal mol^{-1} much larger, but compared to the DQMC values, PBE-MBD* seems to be overshooting in this case.

For S30L-CI, ωB97X-D3 performs better than PW6B95 in terms of MAD (the MD is similar and about zero). Complexes **1** to **22** are the same as those in the S30L, and the observations described for PW6B95-D3 and the various COSMO-RS parameter sets hold for ωB97X-D3. In case of the complexes with counterions, the COSMO-RS(13-fine) parametrization also yields the most consistent results. It does not always give the smallest error, but no outlier is observed.

Our best method combination to compute ΔG_a now consists of PW6B95-D3 gas phase association energies including the three-body dispersion term or ωB97X-D3 energies when counterions are included, HF-3c frequencies to obtain the thermostatistical corrections from energy to free energy, and COSMO-RS with the 2012 parametrization to calculate the solvation free energies for nonpolar solvents, and the 2013-fine parametrization for water and when counterions are included.

This combination yields an MAD of only 2.4 kcal mol^{-1} for the S30L and PW6B95-D3 (2.9 kcal mol^{-1} for the S30L-CI) and 2.1 kcal mol^{-1} for the S30L-CI and ωB97X-D3 (2.6 kcal mol^{-1} for the S30L). When judging this deviation, one should keep in mind that the small ΔG_a values result as a sum of individually large and oppositely signed contributions as discussed already in ref 18 (see Figure 7). The MD for both approaches is almost zero (−0.5 to 0.5 kcal mol^{-1}) indicating the absence of systematic errors (or a very favorable systematic compensation). Because the final ΔG_a values for many (neutral) complexes are rather small (between −5 and −10 kcal mol^{-1}), the mean relative deviation for the whole set is with about 50% rather large. The overall correlation between experiment and theory is reasonable, the Pearson correlation coefficient is R = 0.80 for PW6B95-D3 on S30L and R = 0.89 for ωB97X-D3 on the S30L-CI set. A linear regression gives a slope of 0.93 for S30L/PW6B95-D3 and 0.92 for S30L-CI/ωB97X-D3 indicating only minor systematic deviations.

Figure 7 shows the individual contributions to the total free energy of association exemplary for the method combination PW6B95-D3/HF-3c/COSMO-RS(12/13-fine) for S30L-CI. The pure electronic DFT energy ΔE_{el}^{DFT} ranges from −53.3 kcal mol^{-1} for **23-CI**, which shows nearly pure hydrogen bonding, to almost zero for **11** and **12**, which are mainly bound by dispersion interactions. The two-body dispersion $\Delta E_{disp}^{(2)}$ contribution ranges from −5.2 to −43.9 kcal mol^{-1}. For **22**

DOI: 10.1021/acs.jctc.5b00296
J. Chem. Theory Comput. 2015, 11, 3785−3801

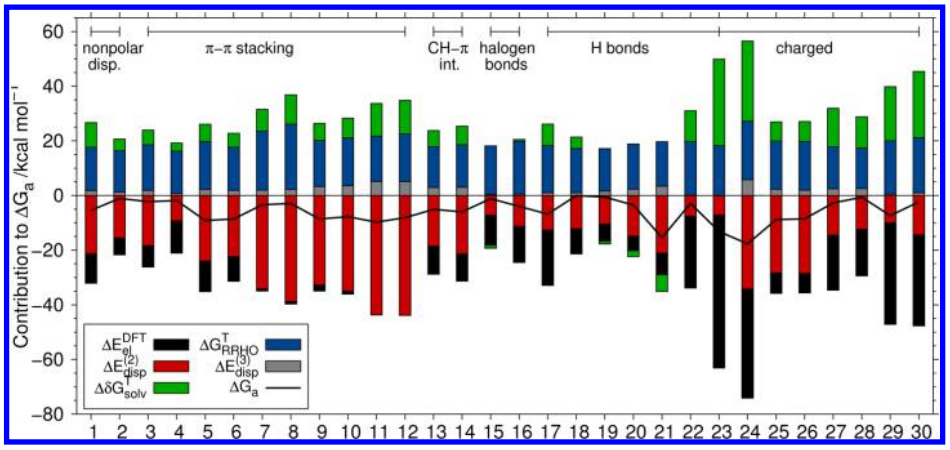

Figure 7. Contributions to ΔG_a for S30L-CI (pure electronic energy (ΔE_{el}^{DFT}), two-body ($\Delta E_{disp}^{(2)}$) and three-body ($\Delta E_{disp}^{(3)}$) dispersion energy, thermal corrections from energy to free energy (ΔG_{RRHO}^{T}), and solvation free energy ($\Delta\delta G_{solv}^{T}$)), and total ΔG_a values for the method combination PW6B95-D3/HF-3c/COSMO-RS(12/13-fine). The lengths of the bars represent the size of the contributions. All values are given in kcal mol^{-1}.

and **23-CI**, which geometrically have a small contact area between host and guest, the $\Delta E_{disp}^{(2)}$ part is about −5 to −7 kcal mol^{-1} smaller compared to that of most other complexes. As we have already shown previously for many supramolecular systems,[18,20,54] the two-body dispersion contribution easily outranks the pure electronic DFT energy. The three-body dispersion term $\Delta E_{disp}^{(3)}$ ranges from almost zero for the nearly planar complexes **22** and **23-CI** up to 5.9 kcal mol^{-1} for **24-CI**. Again, we find that $\Delta E_{disp}^{(3)}$ contributes repulsively with 2 to 3 kcal mol^{-1} on average. The thermal corrections from energy to free energy ΔG_{RRHO}^{T} vary less, between 15 and 20 kcal mol^{-1}. The solvation contribution $\Delta\delta G_{solv}^{T}$ is positive in most cases except for complexes **19**, **20**, and **21** and ranges from −6.2 for **21** to 31.7 kcal mol^{-1} for **23**. As Figure 7 also shows the total ΔG_a values, one can easily see that a large gas phase association energy does not necessarily result in a large association free energy in solution if the solvation contribution is big. Therefore, all parts are significant, and solely ΔE cannot be used to explain binding affinity trends in solution.

In 13 cases, two complexes (deliberately) share the same host molecule. For these systems, relative binding affinities $\Delta\Delta G_a$ were calculated and compared to those of the experiment in order to evaluate if our best method combination is able to correctly reproduce those. The results are shown for PW6B95-D3/HF-3c/COSMO-RS(12/13-fine) in Figure 8. For two pairs of complexes, **3**/**4** and **13**/**14**, the wrong trend is observed. For all others, it is correct, but the differences in binding tend to be overestimated. Compared to the experiment, the MAD for $\Delta\Delta G_a$ is 1.2 kcal mol^{-1}, and the MD is almost zero. This improved accuracy compared to the results for ΔG_a indicates favorable error compensation.

3.4. Binding Energy Reference Values for Benchmarking Purposes. In order to provide convenient gas phase binding energies for benchmarking, we back-correct the experimental binding free energies ΔG_a^{exp} to obtain empirical ("experimental") binding energies ΔE^{emp} as reference values in analogy to the original work for S12L.[18,19] Therefore, we subtract the best thermostatistical corrections calculated with HF-3c and the solvation contributions obtained with COSMO-RS(12) for nonpolar solvents and COSMO-RS(13-fine) for water from the experimental ΔG_a^{exp}:

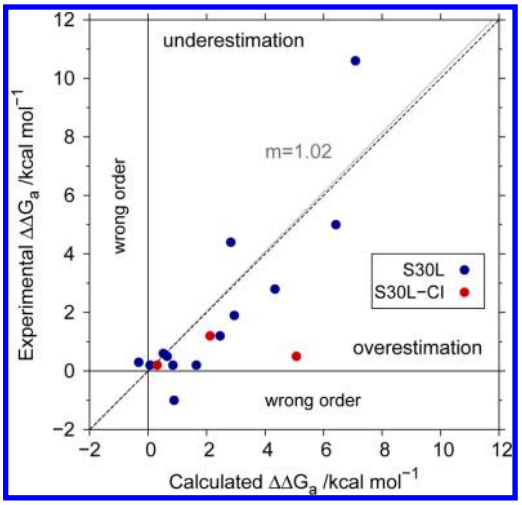

Figure 8. Comparison of experimental $\Delta\Delta G_a^{exp}$ and computed $\Delta\Delta G_a$ for complexes with the same host and different guest molecules on the PW6B95-D3/HF-3c/COSMO-RS(12/13-fine) level. The dashed gray line shows the result of a linear regression for S30L with slope 1.02.

$$\Delta E^{emp} = \Delta G_a^{\exp} - \Delta G_{RRHO}^{T}(\text{HF-3c}) - \Delta\delta G_{solv}^{T}(X)\ (\text{COSMO-RS(12/13-fine)}) \quad (4)$$

These values are collected in Table 2. Since the $\Delta\delta G_{solv}$ values vary for different COSMO-RS parametrizations and we think that the solvation contribution is the least accurate theoretical component, we decided to define our error in ΔE^{emp} as 10% of the chosen $\Delta\delta G_{solv}$ COSMO-RS results. For comparison, the calculated ΔE values on the presumably most accurate DFT level (PW6B95-D3/def2-QZVP′) are provided. Further, a comparison of the two best functionals PW6B95-D3 and ωB97X-D3 with the reference values ΔE^{emp} is shown in Figure 9. Except for the aforementioned outlier **22**, the PW6B95-D3 energies agree well with the back corrected ΔE^{emp}. As noted above, for S30L both data sets have an MAD of 2.4 and 2.8 kcal mol^{-1}, respectively, and for the S30L-CI 2.6 and 2.1 kcal mol^{-1}, respectively. These values should be kept in mind when other theoretical methods are benchmarked against ΔE^{emp}. At present, it seems difficult to guess if the residual errors in the DFT-D3 treatment or the inherent errors in the experimental data and the back-correction scheme are larger. As will be

DOI: 10.1021/acs.jctc.5b00296
J. Chem. Theory Comput. 2015, 11, 3785−3801

Table 2. Empirical Binding Energies ΔE^{emp} for the S30L and S30L-CI Sets Obtained via Back Correcting the Experimental ΔG_a^{exp} Values and Our Best Calculated Binding Energies ΔE^{calc} on the PW6B95-D3/def2-QZVP′ Level for Comparison[a]

	ΔE^{emp}	ΔE^{calc}		ΔE^{emp}	ΔE^{calc}		ΔE^{emp}	ΔE^{calc}
1	−29.0 ± 0.9	−30.2	**14**	−31.3 ± 0.7	−28.28	**27**	−82.2 ± 6.0	−82.1
2	−20.8 ± 0.4	−20.4	**15**	−17.4 ± −0.1	−17.84	**28**	−80.1 ± 6.0	−78.8
3	−23.5 ± 0.5	−24.2	**16**	−25.1 ± 0.1	−24.02	**29**	−53.5 ± 2.6	−54.3
4	−20.3 ± 0.3	−20.3	**17**	−33.4 ± 0.8	−31.87	**30**	−49.3 ± 2.1	−49.9
5	−29.0 ± 0.6	−32.9	**18**	−23.3 ± 0.4	−20.38	**23(CI)**	−67.3 ± 3.2	−63.2
6	−25.5 ± 0.5	−29.5	**19**	−17.5 ± −0.1	−15.01	**24(CI)**	−75.4 ± 2.9	−68.4
7	−35.1 ± 0.8	−32.9	**20**	−19.2 ± −0.2	−17.85	**25(CI)**	−29.1 ± 0.7	−33.5
8	−36.8 ± 1.1	−37.5	**21**	−24.2 ± −0.6	−25.56	**26(CI)**	−29.4 ± 0.7	−33.7
9	−28.4 ± 0.6	−31.7	**22**	−42.6 ± 1.1	−33.79	**27(CI)**	−36.3 ± 1.4	−32.1
10	−29.8 ± 0.7	−32.4	**23**	−61.3 ± 2.6	−58.9	**28(CI)**	−32.0 ± 1.1	−26.9
11	−33.0 ± 1.2	−38.3	**24**	−135.5 ± 8.9	−133.4	**29(CI)**	−47.5 ± 2.0	−46.7
12	−33.9 ± 1.2	−37.8	**25**	−26.0 ± 0.4	−30.5	**30(CI)**	−52.1 ± 2.4	−46.7
13	−30.8 ± 0.6	−25.9	**26**	−25.8 ± 0.4	−30.4			

[a]Complexes of the S30L-CI including counterions are indicated with a "CI". All values are given in kcal mol^{-1}.

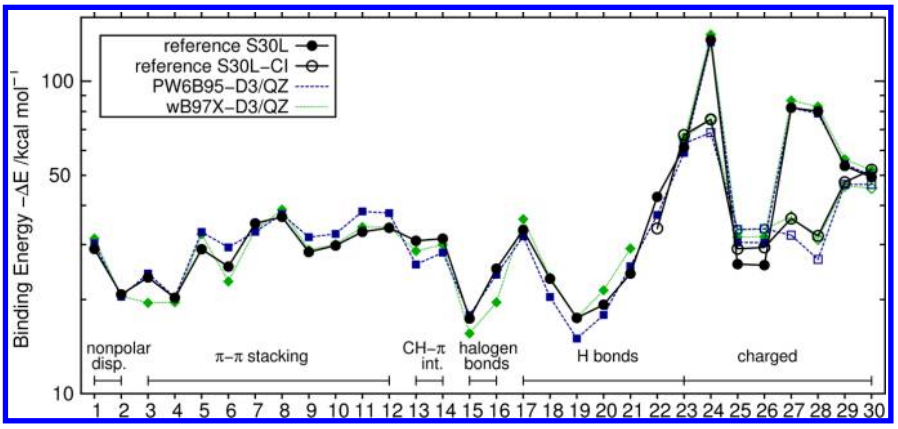

Figure 9. Empirical binding energies ΔE^{emp} in comparison to binding energies for the best functionals PW6B95-D3 and ωB97X-D3 together with a QZ basis set.

shown below, however, the agreement achieved is sufficient to benchmark lower-level quantum chemical methods which are mostly less accurate than the mentioned 3 kcal mol^{-1} uncertainty. This holds even more for common force-field approaches, which are expected to have problems to reach average errors below 10 kcal mol^{-1} for S30L according to some preliminary test calculations.

For some complexes already contained in the old S12L set, diffusion quantum Monte Carlo (DQMC) calculations were performed,[23] and for all of them, symmetry adapted perturbation theory (DFT-SAPT) computations exist.[22] The binding energies obtained with these methods are in good agreement with our new ΔE^{emp}. A table with a direct comparison is provided in the Supporting Information (Table S6). The maximal deviation between ΔE^{emp} and the DQMC and DFT-SAPT results amounts to 2.5 kcal mol^{-1}, which is more than reasonable. This gives us confidence in the back correcting scheme and the choice of $\Delta\delta G_{solv}$ contributions.

Error distributions for the relative deviation from ΔE^{emp} are depicted in Figure 10 for the S30L and all tested functionals. The statistical data (MD, MAD, mean absolute relative deviation (MARD), mean relative deviation (MRD), and standard relative deviation (SRD)) are given in Table 3. Note that all methods including the semiempirical ones are benchmarked as usual by single-point energy computations. The widths (SRD) of the error distributions for PW6B95-D3/QZ, ωB97X-D3/QZ, and PBE-D3/QZ are small with about 10%. B3LYP-D3/QZ, BLYP-D3/QZ, and TPSS-D3/QZ have a broader distribution with widths of about 14−16%. PW6B95-D3/QZ and ωB97X-D3/QZ show no systematic error, whereas PBE-D3/QZ tends to underbind by about 7% on average. TPSS-D3/QZ, B3LYP-D3/QZ, as well as BLYP-D3/QZ exhibit a systematic overbinding by about 5, 10, and 14%,

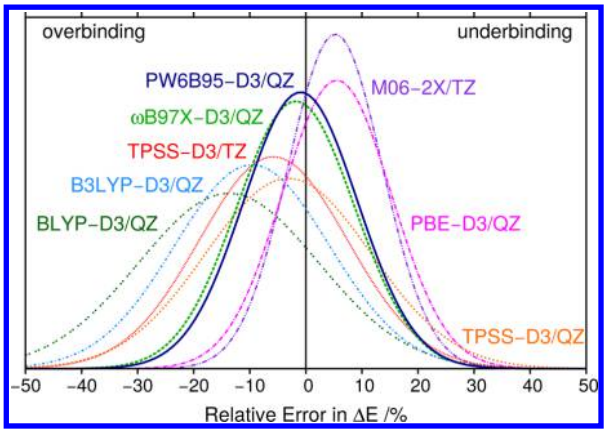

Figure 10. Visualization of the statistical distribution of the relative errors in ΔE with respect to ΔE_{emp} for several functionals for S30L. The half widths of the Gaussians represent the SD, and their shift from the origin corresponds to the MD.

DOI: 10.1021/acs.jctc.5b00296
J. Chem. Theory Comput. 2015, 11, 3785−3801

Table 3. MAD and MD in kcal mol^{-1}, and MARD, MRD, and SRD in % for S30L for Various Functionals Compared to ΔE^{emp} [a]

	MAD	MD	MARD	MRD	SRD
PW6B95-D3/QZ	2.4	−0.1	7.9	0.9	10.1
ωB97X-D3/QZ	2.6	−0.9	8.0	1.8	10.5
B3LYP-D3/QZ	4.1	−2.7	13.2	9.6	13.8
BLYP-D3/QZ	4.8	−4.1	16.0	13.8	16.0
PBE-D3/QZ	2.8	1.8	8.4	−5.5	9.7
TPSS-D3/QZ	3.6	−0.5	11.8	3.1	14.7
TPSS-D3/TZ	3.5	−1.6	11.1	5.8	13.2
M06-2X/TZ	2.5	1.4	8.1	−5.2	8.4
M06-2X-D3/TZ	4.8	−4.4	15.0	13.5	10.0

[a]A negative MD means overbinding, and a positive MD means underbinding.

respectively. TPSS-D3-/TZ performs similar to TPSS-D3/QZ with a bit worse MD and MRD and slightly better MAD, MARD, and SRD.

Because the Minnesota functionals[104] include medium-range dispersion effects and are widely used for noncovalently bound systems, we tested the prototypical M06-2X functional also at the TZ basis set level so that the results are directly comparable to TPSS-D3/TZ. M06-2X/TZ yields a smaller standard deviation than TPSS-D3/TZ of about 8% and tends to underbind by about 5% similar to TPSS-D3/TZ. Adding the D3(0)+ATM corrections yields overbinding by about 14% on average indicating the appearance of the residual BSSE.

3.5. Performance of Semiempirical Methods. The empirical binding energies ΔE^{emp} were used to benchmark the performance of various semiempirical (minimal basis set) methods which are typically about 2 to 3 orders of magnitude faster than DFT/"large basis" calculations. Thus, these methods can be used for, e.g., prescreening of different possible conformers or binding modes in supramolecular complexes if they yield sufficiently accurate binding energies.

We tested HF-3c, DFTB-D3, PM6-D3, and PM6-D3 in combination with hydrogen bonding corrections of second generation H2[116] (PM6-D3H2), third generation H+[119] (PM6-D3H+), and fourth generation H4[120] (PM6-D3H4), as well as PM7[117] and OM2-D3.[121] For the semiempirical methods, the abbreviation D3 does not include the three-body dispersion. If the ATM term is included, it is stated explicitly. In the case of PM6, the zero damping for the D3 correction was used throughout, as the hydrogen bonding corrections were parametrized in this way. Of all the methods tested, HF-3c is the most expensive one because all integrals are computed (about 50 times slower than the "truly" semiempirical PMX or OMX methods). Nevertheless, HF-3c calculations can be carried out routinely on a standard workstation for hundreds to about 1000 atoms.

The MADs (and MDs) with respect to ΔE^{emp} are given in Figure 11 for the S30L and S30L-CI sets and with and without inclusion of the three-body dispersion. OM2 has no parameters for sodium, sulfur, chlorine, and iodine, and hence, no results could be obtained for the complexes **4**, **11**, **12**, **14**, **15**, **16** and all complexes including counterions (**23-CI** to **30-CI**). Thus, for S30L-CI half of the complexes could not be treated, and we disregarded the statistical analysis for S30L-CI with OM2-D3.

With the sole exception of PM7 (which shows a huge MAD of about 15 kcal mol^{-1}), all tested semiempirical methods can be recommended and in particular for neutral systems. Methods like PM6-D3H2 treat the dispersion and hydrogen bonding corrections independently of PM6, whereas for PM7 explicit terms for dispersion and hydrogen bonding are included in the method itself and optimized during the parameter fit. PM7 performs well for small organic complexes like in the S22[138] and S66[139] test sets but still slightly worse than, e.g., PM6-DH2.[117,140,141] This result clearly shows that the PM7 parameters obtained for small systems cannot easily be used to describe the interactions in large supramolecular complexes. OM2-D3 also shows a large MAD of about 10 kcal mol^{-1}. This is due to the bad description of the anionic systems **29** and **30**. For these two complexes, ΔE is off by a factor of 2 (overbinding). If **29** and **30** are disregarded from the statistics, the MAD drops to a reasonable value of 5.3 kcal mol^{-1}.

For the S30L set, PM6-D3H2 yields the lowest MAD of 5.7 kcal mol^{-1}. PM6-D3H+, PM6-D3, HF-3c, and DFTB-D3 show similar results ranging from 6.4 to 6.9 kcal mol^{-1}. PM6-D3H4 performs worse than PM6-D3 in combination with the other two hydrogen bond corrections tested and yields a larger MAD of 8.4 kcal mol^{-1}.

As discussed for the DFT methods above, one can see a general improvement of the interaction energies when chloride counterions are used, except for HF-3c for which the MAD and MD almost stay the same. Furthermore, all methods benefit from the inclusion of the three-body dispersion. For DFTB-D3 and all PM6 based methods, the results obtained with counterions and inclusion of the three-body dispersion contribution yield the smallest MADs compared to ΔE^{emp}. The MADs for these six methods range from 3.9 kcal mol^{-1}

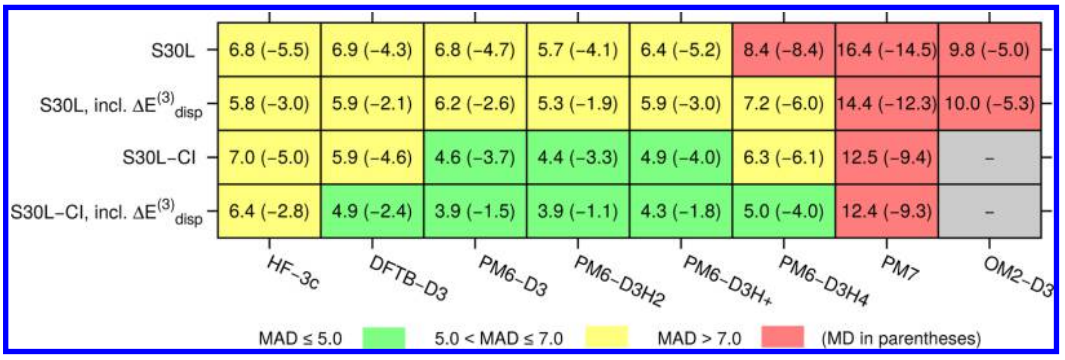

Figure 11. MADs (and MDs) for calculated ΔE of S30L and S30L-CI for several semiempirical methods w.r.t. ΔE^{emp} in kcal mol^{-1}. The values are given with and without inclusion of the three-body dispersion term $\Delta E^{(3)}_{disp}$. For OM2-D3, six complexes had to be disregarded due to missing parameters.

DOI: 10.1021/acs.jctc.5b00296
J. Chem. Theory Comput. 2015, 11, 3785−3801

(PM6-D3) to 5.0 kcal mol^{-1} (PM6-D3H4). PM6-D3H2 and PM6-D3H+ perform similar to plain PM6-D3, and PM6-D3H4 performs worse. HF-3c has a larger MAD of 6.2 kcal mol^{-1}, which is mainly caused by the larger error for the halogen bonded systems **15** and **16** and the anionic ones **29**/**29-CI** and **30**/**30-CI**. For all methods, the MDs are small and negative and lie between −1.1 (PM6-D3H2) and −4.0 kcal mol^{-1} (PM6-D3H4), showing a slight to small systematic overestimation of the binding energies.

The improvement gained with the various hydrogen bonding corrections compared to plain PM6-D3 for the whole set of complexes is small and in most cases negligible. PM6-D3H4 seems to perform generally a bit worse than plain PM6-D3. For the complexes whose interactions are dominated by hydrogen bonding (**17** to **23**), association energies obtained with PM6-D3 and PM6-D3 in combination with any hydrogen bonding correction differ by 3 kcal mol^{-1} at most. We could not identify a version that clearly outperforms the others or is better than PM6-D3 for all of these seven complexes. This was observed before for smaller model complexes as contained in, e.g., the S66[139] or JSCH[138] test sets.[142]

3.6. Semiempirical Methods for Structure Optimization. Finally, we compare the geometries of the complexes obtained with HF-3c, DFTB-D3, PM6-D3, PM6-D3H4, and PM7 with the ones obtained from TPSS-D3/def2-TZVP optimizations taken as reference. We left out OM2 because of convergence problems and PM6-D3H2 due to known small errors in the H2 gradient.[116] DFTB-D3 cannot be applied to the S30L-CI set due to the missing COSMO implementation in the DFTB+ code. As a quality measure, the average root-mean-square deviation ($\overline{\text{RMSD}}$) of the heavy atom coordinates and the mean relative deviation (MRD), and the mean absolute relative deviation (MARD) of the rotational constants were calculated (see Figure 12). For the rotational constants, we

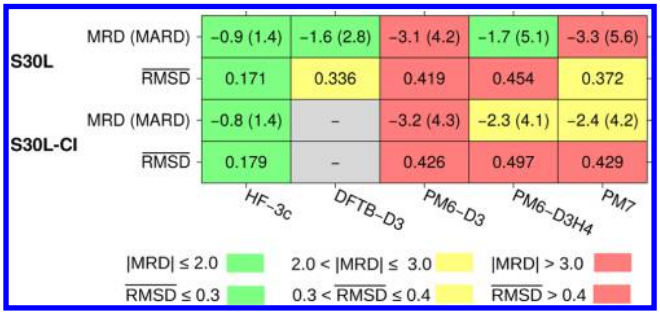

Figure 12. Averaged RMSD ($\overline{\text{RMSD}}$) in Å for the heavy atoms and the MRD (and MARD) of the rotational constants in % w.r.t. TPSS-D3/def2-TZVP geometries for S30L and S30L-CI. For the rotational constants, a negative MRD corresponds to a structure with a too small spatial extent.

define the error as $B_{semiemp.} - B_{TPSS-D3/def2-TZVP}$ so that a negative MRD denotes a structure with too small spatial extent. One has to keep in mind that TPSS-D3 structures have small errors themselves, but better hybrid DFT (or MP2 for saturated complexes) cannot be obtained routinely for such large systems which require typically hundreds of structure optimization steps. In general, for small noncovalent complexes DFT-D3 yields reasonable geometries.[143] For small covalently bound organic molecules, TPSS-D3 yields geometries with slightly too large spatial extent.[144]

All tested semiempirical methods except PM7 yield very similar $\overline{\text{RMSD}}$s for the complexes with counterions included and for those without. For PM7, the $\overline{\text{RMSD}}$ increases by about 0.06 Å. HF-3c yields by far the smallest $\overline{\text{RMSD}}$ of 0.171 Å for S30L, which is about half the magnitude of the values observed for all other tested semiempirical methods. These give values in the range of 0.336 Å (DFTB-D3) up to 0.454 Å (PM6-D3H4). The good agreement of HF-3c and DFT-D3/TZ structures has been observed before.[44,145] Note that PM7 yielded the worst association energies, but the geometries are as good as DFTB-D3 and (hydrogen bonding corrected) PM6-D3 results.

Regarding the rotational constants, HF-3c yields the best results with the smallest MRD of −0.9% and the smallest MARD of 1.4%. DFTB-D3 and PM6-D3H4 perform a bit worse for the MRD (−1.6 to −1.7%), and PM6-D3 and PM7 yield much larger MRDs above 3%. The MARDs are at least twice as large as for HF-3c and range from 2.8% for DFTB-D3 to 5.6% for PM7. For HF-3c and PM6-D3, the mean relative deviation of the rotational constants does not change much when counterions are included. In the case of PM6-D3H4, a deterioration of 0.5% and in case of PM7 an improvement of 0.9% are observed. Overall, we find that HF-3c yields the most accurate geometries of all tested semiempirical methods, which agrees well with our previous finding that HF-3c yields the best thermostatistical corrections.

4. CONCLUSIONS

The S12L test set for supramolecular association free energies ΔG_a was extended to 30 complexes (S30L). It features complexes with higher charges (up to +4) and anions (−1), slightly less rigid hosts, more diverse types of noncovalent interactions, and larger system sizes (up to 200 atoms). The ΔG_a values were obtained in a nonempirical, static single structure approach by adding the computed gas phase binding energy, the thermostatistical corrections from energy to free energy, and the solvation free energy.

Various dispersion corrected density functionals (PW6B95-D3, B3LYP-D3, TPSS-D3, PBE-D3, and ωB97X-D3) in combination with a quadruple-ζ basis set were tested for calculating the association energies in the gas phase including our standard Axilrod−Teller−Muto type three-body dispersion correction. Various minimal basis set and semiempirical methods (HF-3c, PM6-D3, and DFTB-D3) were used to obtain the thermostatistical contributions. Several versions of the COSMO-RS model as well as SMD were employed to include solvation effects. In order to find the best procedure to predict theoretical ΔG_a values, we investigated and statistically analyzed all possible combinations of these methods. The best performing density functional and the best method for thermostatistical corrections could be clearly identified, whereas for the solvation free energies many COSMO-RS parametrizations perform similarly. When looking closer, we found that the COSMO-RS(12) parameters perform best and most consistently for nonpolar solvents, whereas for water COSMO-RS(13-fine) yields better results. Thus, the proposed method combination consists of PW6B95-D3/def2-QZVP′ energies on TPSS-D3/def2-TZVP optimized geometries, HF-3c thermostatistical corrections, and COSMO-RS(12/13-fine) (for nonpolar solvents/water) solvation free energies.

Further, we investigated the effect of counterions for the charged systems (S30L-CI) on the gas phase binding energy calculations as well as on the solvation term. The inclusion of counterions reduced the error in most cases for the cationic

DOI: 10.1021/acs.jctc.5b00296
J. Chem. Theory Comput. 2015, 11, 3785−3801

systems and is thus recommended as a default procedure. For the association energies, ωB97X-D3 slightly outperforms PW6B95-D3 and thus is advised for charged systems. In the case of the solvation term, the COSMO-RS(13-fine) parametrization again works best. Our best method combinations give a mean absolute deviation of only 2.4 kcal mol^{-1} for S30L (PW6B95-D3) and 2.1 kcal mol^{-1} for S30L-CI (ωB97X-D3) and a mean deviation of almost zero compared to experimental ΔG_a^{exp}.

Thirteen pairs of complexes (deliberatly) share the same host. For those relative association free energies were calculated in order to evaluate if the correct trend in binding affinities is observed. Except for two cases, this always is the case. The MAD compared to experiment amounts to 1.2 kcal mol^{-1}, and the MD is almost zero.

The thermostatistical and solvation data above were used to back-correct the experimental association free energies from solution measurements in order to get an empirical estimate for the "experimental" binding energies in the gas phase as done previously for the S12L set. These reference data are utilized to benchmark the performance of various semiempirical, minimal basis set methods for binding energies. HF-3c, DFTB-D3, OM2, PM6-D3 (with and without various hydrogen bonding corrections), and PM7 were tested. Apart from PM7 (whose errors are huge), all of these methods perform rather similarly, although clearly worse than dispersion corrected DFT/"large basis set". They can be recommended in general for neutral complexes. For charged systems, the "simple" methods perform less well, and their application in such cases requires careful testing on the specific problem under consideration. The choice of the hydrogen bonding correction for PM6-D3 has no significant impact. Again, inclusion of counterions improves the semiempirical results and so does the three-body dispersion term.

Finally, we investigated the geometries of the complexes obtained with the semiempirical methods. HF-3c yields the by far smallest averaged RMSD of 0.18 Å compared to TPSS-D3/def2-TZVP reference data. All other methods perform similarly and give RMSDs in the range of 0.34 Å (DFTB-D3) up to 0.45 Å (PM6-D3H4). This picture changes only slightly in favor of PM6-D3H4 when rotational constants are used to measure the quality of the structures.

In summary, the future for the prediction and understanding of supramolecular interactions by dispersion corrected DFT seems bright. If the structures are not too flexible and only a few conformers have to be considered, reasonably accurate absolute as well as relative binding affinities can be computed routinely. We found no indications in S30L that slightly more flexible complexes exhibit larger errors but note that extended π-systems seem to be somewhat problematic in the gas phase interaction part. The small residual deviations of 2−3 kcal/mol (typically 5−10% of ΔE) are impressive for large complexes with 200 atoms from a theoretical point of view. However, achieving "chemical accuracy" at a 1 kcal mol^{-1} level for ΔG_a seems to be extremely difficult and likely requires improvement of gas phase interaction energies, inclusion of anharmonic and dynamic effects as well as a much more accurate solvation treatment.

■ ASSOCIATED CONTENT

Supporting Information

TPSS-D3/def2-TZVP geometries of all complexes as Cartesian coordinates, all individual contributions to ΔG_a (ΔE, ΔG_{RRHO}^T, and $\Delta\delta\ G_{solv}^T$) for all used methods, and additional statistical analyses. The Supporting Information is available free of charge on the ACS Publications website at DOI: 10.1021/acs.jctc.5b00296.

■ AUTHOR INFORMATION

Corresponding Author

*Phone: +49 0-228-73-2351. Fax: +49-0-228-73-9064. E-mail: grimme@thch.uni-bonn.de.

Funding

We thank A. Hansen for helpful discussions, G. Brandenburg for technical support regarding the H+ hydrogen bonding corrections for the PM6-D3 method, and A. Goeller (Bayer AG) for comparing our SMD values to those he obtained with Gaussian.

Notes

The authors declare no competing financial interest.

■ REFERENCES

(1) Kim, K. S.; Tarakeshwar, P.; Lee, J. Y. *Chem. Rev.* **2000**, *100*, 4145−4186.
(2) Riley, K. E.; Hobza, P. *WIREs Comput. Mol. Sci.* **2011**, *1*, 3−17.
(3) Hohenstein, E. G.; Sherrill, C. D. *WIREs Rev. Comput. Mol. Sci.* **2012**, *2*, 304−326.
(4) Lehn, J.-M. *Supramolecular Chemistry: Concepts and Perspectives*; VCH: Weinheim, Germany, 1995.
(5) Atwood, J. L., Steed, J. *Supramolecular Chemistry*, 2nd ed.; Wiley: West Sussex, U.K., 2009.
(6) Stone, A. J. *The Theory of Intermolecular Forces*; Oxford University Press: Oxford, U.K., 1997.
(7) Lehn, J.-M. *Angew. Chem., Int. Ed.* **1988**, *27*, 89−112.
(8) Cram, D. J. *Angew. Chem., Int. Ed.* **1988**, *27*, 1009−1020.
(9) Lehn, J. *Science* **1993**, *260*, 1762−1763.
(10) Kristyán, S.; Pulay, P. *Chem. Phys. Lett.* **1994**, *229*, 175−180.
(11) Hobza, P.; Šponer, J.; Reschel, T. *J. Comput. Chem.* **1995**, *16*, 1315−1325.
(12) Pérez-Jordá, J.; Becke, A. *Chem. Phys. Lett.* **1995**, *233*, 134−137.
(13) Grimme, S. *WIREs Comput. Mol. Sci.* **2011**, *1*, 211−228.
(14) Jiri, K.; Michaelides, A. *J. Chem. Phys.* **2012**, *137*, 120901.
(15) Burns, L. A.; Vázquez-Mayagoitia, A.; Sumpter, B. G.; Sherrill, C. D. *J. Chem. Phys.* **2011**, *134*, 084107.
(16) Goerigk, L. *J. Chem. Theory Comput.* **2014**, *10*, 968−980.
(17) Grimme, S.; Antony, J.; Ehrlich, S.; Krieg, H. *J. Chem. Phys.* **2010**, *132*, 154104.
(18) Grimme, S. *Chem.—Eur. J.* **2012**, *18*, 9955−9964.
(19) Risthaus, T.; Grimme, S. *J. Chem. Theory Comput.* **2013**, *9*, 1580−1591.
(20) Antony, J.; Sure, R.; Grimme, S. *Chem. Commun.* **2015**, *51*, 1764−1774.
(21) Ohlendorf, G.; Mahler, C. W.; Jester, S.-S.; Schnakenburg, G.; Grimme, S.; Höger, S. *Angew. Chem., Int. Ed.* **2013**, *52*, 12086−12090.
(22) Heßelmann, A.; Korona, T. *J. Chem. Phys.* **2014**, *141*, 094107.
(23) Ambrosetti, A.; Alfè, D.; DiStasio, R. A.; Tkatchenko, A. *J. Phys. Chem. Lett.* **2014**, *5*, 849−855.
(24) Sedlak, R.; Janowski, T.; Pitoňák, M.; Rezáč, J.; Pulay, P.; Hobza, P. *J. Chem. Theory Comput.* **2013**, *9*, 3364−3374.
(25) Tao, J.; Perdew, J.; Staroverov, V.; Scuseria, G. *Phys. Rev. Lett.* **2003**, *91*, 146401.
(26) Weigend, F.; Ahlrichs, R. *Phys. Chem. Chem. Phys.* **2005**, *7*, 3297−305.
(27) Johnson, E. R.; Becke, A. D. *J. Chem. Phys.* **2005**, *123*, 24101.
(28) Becke, A. D.; Johnson, E. R. *J. Chem. Phys.* **2005**, *123*, 154101.
(29) Grimme, S.; Ehrlich, S.; Goerigk, L. *J. Comput. Chem.* **2011**, *32*, 1456−1465.
(30) Zhao, Y.; Truhlar, D. G. J. *J. Phys. Chem. A* **2005**, *109*, 5656−5667.

DOI: 10.1021/acs.jctc.5b00296
J. Chem. Theory Comput. 2015, 11, 3785−3801

(31) Tkatchenko, A.; Alfè, D.; Kim, K. S. *J. Chem. Theory Comput.* **2012**, *8*, 4317−4322.
(32) DiStasio, R. A., Jr.; Gobre, V. V.; Tkatchenko, A. *J. Phys.: Condens. Matter* **2014**, *26*, 213202.
(33) Kennedy, M. R.; McDonald, A. R.; DePrince, A. E.; Marshall, M. S.; Podeszwa, R.; Sherrill, C. D. *J. Chem. Phys.* **2014**, *140*, 121104.
(34) Tkatchenko, A. *Adv. Funct. Mater.* **2014**, *25*, 1054−2061.
(35) Dobson, J. F. *Int. J. Quantum Chem.* **2014**, *114*, 1157−1161.
(36) Tkatchenko, A.; DiStasio, R. A.; Car, R.; Scheffler, M. *Phys. Rev. Lett.* **2012**, *108*, 236402.
(37) Moellmann, J.; Grimme, S. *J. Phys. Chem. C* **2014**, *118*, 7615−7621.
(38) Brandenburg, J. G.; Maas, T.; Grimme, S. *J. Chem. Phys.* **2015**, *142*, 124104.
(39) Qu, Z.-W.; Hansen, A.; Grimme, S. *J. Chem. Theory Comput.* **2015**, *11*, 1037−1045.
(40) Bannwarth, C.; Hansen, A.; Grimme, S. *Isr. J. Chem.* **2015**, *55*, 235−242.
(41) Hansen, A.; Bannwarth, C.; Grimme, S.; Petrović, P.; Werlé, C.; Djukic, J.-P. *ChemistryOpen* **2014**, *3*, 177−189.
(42) Stewart, J. J. P. *J. Mol. Model.* **2007**, *13*, 1173−1213.
(43) Elstner, M.; Porezag, D.; Jungnickel, G.; Elsner, J.; Haugk, M.; Frauenheim, T.; Suhai, S.; Seifert, G. *Phys. Rev. B* **1998**, *58*, 7260−7268.
(44) Sure, R.; Grimme, S. *J. Comput. Chem.* **2013**, *34*, 1672−1685.
(45) Kruse, H.; Grimme, S. *J. Chem. Phys.* **2012**, *136*, 154101.
(46) Klamt, A. *J. Phys. Chem.* **1995**, *99*, 2224−2235.
(47) Eckert, F.; Klamt, A. *AIChE J.* **2002**, *48*, 369−385.
(48) Marenich, A. V.; Cramer, C. J.; Truhlar, D. G. *J. Phys. Chem. B* **2009**, *113*, 6378−6396.
(49) Kloss, T.; Heil, J.; Kast, S. M. *J. Phys. Chem. B* **2008**, *112*, 4337−4343.
(50) Hoffgaard, F.; Heil, J.; Kast, S. M. *J. Chem. Theory Comput.* **2013**, *9*, 4718−4726.
(51) Fenley, A. T.; Henriksen, N. M.; Muddana, H. S.; Gilson, M. K. *J. Chem. Theory Comput.* **2014**, *10*, 4069−4078.
(52) Nguyen, C. N.; Cruz, A.; Gilson, M. K.; Kurtzman, T. *J. Chem. Theory Comput.* **2014**, *10*, 2769−2780.
(53) See http://sampl.eyesopen.com/.
(54) Sure, R.; Antony, J.; Grimme, S. *J. Phys. Chem. B* **2014**, *118*, 3431−3440.
(55) Muddana, H. S.; Fenley, A. T.; Mobley, D. L.; Gilson, M. K. *J. Comput.-Aided Mol. Des.* **2014**, *28*, 305−17.
(56) Ehrlich, S.; Moellmann, J.; Grimme, S. *Acc. Chem. Res.* **2013**, *46*, 916−926.
(57) Kamieth, M.; Burkert, U.; Corbin, P. S.; Dell, S. J.; Zimmerman, S. C.; Klärner, F.-G. *Eur. J. Org. Chem.* **1999**, 2741−2749.
(58) Graton, J.; le Questel, J.-Y.; Legouin, B.; Uriac, P.; van de Weghe, P.; Jacquemin, D. *Chem. Phys. Lett.* **2012**, *522*, 11−16.
(59) Petitjean, A.; Khoury, R. G.; Kyritsakas, N.; Lehn, J.-M. *J. Am. Chem. Soc.* **2004**, *126*, 6637−6647.
(60) Kawase, T.; Nishiyama, Y.; Nakamura, T.; Ebi, T.; Matsumoto, K.; Kurata, H.; Oda, M. *Angew. Chem., Int. Ed.* **2007**, *46*, 1086−8.
(61) Mück-Lichtenfeld, C.; Grimme, S.; Kobryn, L.; Sygula, A. *Phys. Chem. Chem. Phys.* **2010**, *12*, 7091−7097.
(62) Georghiou, P. E.; Tran, A. H.; Mizyed, S.; Bancu, M.; Scott, L. T. *J. Org. Chem.* **2005**, *70*, 6158−63.
(63) Hornung, J.; Fankhauser, D.; Shirtcliff, L. D.; Praetorius, A.; Schweizer, W. B.; Diederich, F. *Chem.—Eur. J.* **2011**, *17*, 12362−71.
(64) Jungbauer, S. H.; Bulfield, D.; Kniep, F.; Lehmann, C. W.; Herdtweck, E.; Huber, S. M. *J. Am. Chem. Soc.* **2014**, *136*, 16740−3.
(65) Allott, C.; Adams, H.; Hunter, C. A.; Thomas, J. A.; Bernad, P. L., Jr.; Rotger, C. *Chem. Commun.* **1998**, 2449−2450.
(66) Liu, Y.; Yang, E.-C.; Yang, Y.-W.; Zhang, H.-Y.; Fan, Z.; Ding, F.; Cao, R. *J. Org. Chem.* **2004**, *69*, 173−80.
(67) Moghaddam, S.; Yang, C.; Rekharsky, M.; Ko, Y. H.; Kim, K.; Inoue, Y.; Gilson, M. K. *J. Am. Chem. Soc.* **2011**, *133*, 3570−81.
(68) Park, T.; Zimmerman, S. C.; Nakashima, S. *J. Am. Chem. Soc.* **2005**, *127*, 6520−1.
(69) Blight, B. A.; Hunter, C. A.; Leigh, D. A.; McNab, H.; Thomson, P. I. T. *Nat. Chem.* **2011**, *3*, 244−48.
(70) Cao, L.; Sekutor, M.; Zavalij, P. Y.; Mlinarić-Majerski, K.; Glaser, R.; Isaacs, L. *Angew. Chem., Int. Ed.* **2014**, *53*, 988−93.
(71) Juríček, M.; Barnes, J. C.; Dale, E. J.; Liu, W.-G.; Strutt, N. L.; Bruns, C. J.; Vermeulen, N. A.; Ghooray, K. C.; Sarjeant, A. A.; Stern, C. L.; Botros, Y. Y.; Goddard, W. A.; Stoddart, J. F. *J. Am. Chem. Soc.* **2013**, *135*, 12736−46.
(72) Mock, W. L.; Shih, N. Y. *J. Am. Chem. Soc.* **1989**, *111*, 2697−2699.
(73) Chang, K.-C.; Minami, T.; Koutnik, P.; Savechenkov, P. Y.; Liu, Y.; Anzenbacher, P. *J. Am. Chem. Soc.* **2014**, *136*, 1520−5.
(74) Feringa, B. L. *Molecular Switches*, 2nd ed.; Wiley-VCH: Weinheim, Germany, 2011.
(75) Ugarte, D. *Nature* **1992**, *359*, 707−9.
(76) Smith, B. W.; Monthioux, M.; Luzzi, D. E. *Nature* **1998**, *396*, 323−324.
(77) Kroto, H. W.; McKay, K. *Nature* **1988**, *331*, 328−331.
(78) Kawase, T.; Tanaka, K.; Fujiwara, N.; Darabi, H. R.; Oda, M. *Angew. Chem. Int. Ed.* **2003**, *42*, 1624−8.
(79) Wolters, L. P.; Schyman, P.; Pavan, M. J.; Jorgensen, W. L.; Bickelhaupt, F. M.; Kozuch, S. *WIREs Comput. Mol. Sci.* **2014**, *4*, 523−540.
(80) Riley, K. E.; Hobza, P. *Phys. Chem. Chem. Phys.* **2013**, *15*, 17742−51.
(81) Kozuch, S.; Martin, J. M. L. *J. Chem. Theory Comput.* **2013**, *9*, 1918−1931.
(82) Rekharsky, M. V.; Inoue, Y. *Chem. Rev.* **1998**, *98*, 1875−1918.
(83) Lee, J. W.; Samal, S.; Selvapalam, N.; Kim, H.-J.; Kim, K. *Acc. Chem. Res.* **2003**, *36*, 621−30.
(84) Lagona, J.; Mukhopadhyay, P.; Chakrabarti, S.; Isaacs, L. *Angew. Chem., Int. Ed.* **2005**, *44*, 4844−70.
(85) Liu, S.; Ruspic, C.; Mukhopadhyay, P.; Chakrabarti, S.; Zavalij, P. Y.; Isaacs, L. *J. Am. Chem. Soc.* **2005**, *127*, 15959−67.
(86) Rekharsky, M. V.; Mori, T.; Yang, C.; Ko, Y. H.; Selvapalam, N.; Kim, H.; Sobransingh, D.; Kaifer, A. E.; Liu, S.; Isaacs, L.; Chen, W.; Moghaddam, S.; Gilson, M. K.; Kim, K.; Inoue, Y. *Proc. Nat. Acad. Sci. U.S.A.* **2007**, *104*, 20737−42.
(87) Liu, S.; Ruspic, C.; Mukhopadhyay, P.; Chakrabarti, S.; Zavalij, P. Y.; Isaacs, L. *J. Am. Chem. Soc.* **2005**, *127*, 15959−67.
(88) Klamt, A.; Schüürmann, G. *J. Chem. Soc. Perkin Trans. 2* **1993**, 799−805.
(89) Benitez, D.; Tkatchouk, E.; Yoon, I.; Stoddart, J. F.; Goddard, W. A. *J. Am. Chem. Soc.* **2008**, *130*, 14928−9.
(90) Iali, W.; Petrović, P.; Pfeffer, M.; Grimme, S.; Djukic, J.-P. *Dalton trans.* **2012**, *41*, 12233−122343.
(91) Becke, A. D. *J. Chem. Phys.* **1993**, *98*, 5648.
(92) Lee, C.; Yang, W.; Parr, R. G. *Phys. Rev. B* **1988**, *37*, 785−789.
(93) Vosko, S. H.; Wilk, L.; Nusair, M. *Can. J. Phys.* **1980**, *58*, 1200−1211.
(94) Stephens, P. J.; Devlin, F. J.; Chabalowski, C. F.; Frisch, M. J. *J. Phys. Chem.* **1994**, *98*, 11623−11627.
(95) Becke, A. D. *Phys. Rev. A* **1988**, *38*, 3098−3100.
(96) Perdew, J. P.; Burke, K.; Ernzerhof, M. *Phys. Rev. Lett.* **1996**, *77*, 3865−3868.
(97) Perdew, J. P.; Burke, K.; Ernzerhof, M. *Phys. Rev. Lett.* **1997**, *78*, 1396−1396.
(98) Lin, Y.-S.; Li, G.-D.; Mao, S.-P.; Chai, J.-D. *J. Chem. Theory Comput.* **2013**, *9*, 263−272.
(99) Peterson, K. A.; Figgen, D.; Goll, E.; Stoll, H.; Dolg, M. *J. Chem. Phys.* **2003**, *119*, 11113−11123.
(100) Ahlrichs, R.; Armbruster, M. K.; Bär, M.; Baron, H.-P.; Bauernschmitt, R.; Crawford, N.; Deglmann, P.; Ehrig, M.; Eichkorn, K.; Elliott, S.; Furche, F.; Haase, F.; Häser, M.; Hättig, C.; Hellweg, A.; Horn, H.; Huber, C.; Huniar, U.; Kattannek, M.; Kölmel, C.; Kollwitz, M.; May, K.; Nava, P.; Ochsenfeld, C.; Öhm, H.; Patzelt, H.; Rappoport, D.; Rubner, O.; Schäfer, A.; Schneider, U.; Sierka, M.; Treutler, O.; Unterreiner, B.; von Arnim, M.; Weigend, F.; Weis, P.;

DOI: 10.1021/acs.jctc.5b00296
J. Chem. Theory Comput. 2015, 11, 3785−3801

Weiss, H. *TURBOMOLE 6.4*; Universität Karlsruhe: Karlsruhe, Germany, 2012. See also: http://www.turbomole.com.
(101) Furche, F.; Ahlrichs, R.; Hättig, C.; Klopper, W.; Sierka, M.; Weigend, F. *WIREs Comput. Mol. Sci.* **2014**, *4*, 91−100.
(102) Neese, F. *ORCA: An ab Initio, Density Functional and Semiempirical Program Package*, version 3.0 (Current Development Version); Max Planck Institute for Chemical Energy Conversion: Mülheim, Germany, 2014.
(103) Neese, F. *WIREs Comput. Mol. Sci.* **2012**, *2*, 73−78.
(104) Zhao, Y.; Truhlar, D. G. *Theor. Chem. Acc.* **2008**, *120*, 215−241.
(105) Eichkorn, K.; Treutler, O.; Öhm, H.; Häser, M.; Ahlrichs, R. *Chem. Phys. Lett.* **1995**, *242*, 652−660.
(106) Weigend, F. *Phys. Chem. Chem. Phys.* **2006**, *8*, 1057−65.
(107) Treutler, O.; Ahlrichs, R. *J. Chem. Phys.* **1995**, *102*, 346−354.
(108) See http://www.thch.uni-bonn.de/tc/.
(109) Kind, C.; Reiher, M.; Neugebauer, J.; Hess, B. A. *SNF*, version 2.2.1; Universität Erlangen: Erlangen, Germany, 2002.
(110) Aradi, B.; Hourahine, B.; Frauenheim, T. *J. Phys. Chem. A* **2007**, *111*, 5678−84.
(111) Yang, Y.; Yu, H.; York, D.; Cui, Q.; Elstner, M. *J. Phys. Chem. A* **2007**, *111*, 10861−73.
(112) Elstner, M. *Theor. Chem. Acc.* **2005**, *116*, 316−325.
(113) Elstner, M. *J. Phys. Chem. A* **2007**, *111*, 5614−21.
(114) Elstner, M. See http://www.dftb.org/.
(115) Brandenburg, J. G.; Grimme, S. *J. Phys. Chem. Lett.* **2014**, *5*, 1785−1789.
(116) Korth, M.; Pitoňák, M.; Rezáč, J.; Hobza, P. *J. Chem. Theory Comput.* **2010**, *6*, 344−352.
(117) Stewart, J. J. P. *J. Mol. Model.* **2013**, *19*, 1−32.
(118) Stewart, J. J. P. *MOPAC2012*;Stewart Computational Chemistry: Colorado Springs, CO, 2012. See http://OpenMOPAC.net.
(119) Korth, M. *J. Chem. Theory Comp.* **2010**, *6*, 3808−3816.
(120) Řezáč, J.; Hobza, P. *J. Chem. Theory Comput.* **2012**, *8*, 141−151.
(121) Weber, W.; Thiel, W. *Theor. Chem. Acc.* **2000**, *103*, 495−506.
(122) Thiel, W. *MNDO2005*, version 7.0; MPI für Kohlenforschung: Mülheim, Germany, 2005.
(123) Eckert, F.; Klamt, A. *COSMOtherm*, version C3.0, release 14.01; COSMOlogic GmbH & Co. KG: Leverkusen, Germany, 2014.
(124) Perdew, J. P. *Phys. Rev. B* **1986**, *33*, 8822−8824.
(125) Schäfer, A.; Huber, C.; Ahlrichs, R. *J. Chem. Phys.* **1994**, *100*, 5829−5235.
(126) Rappoport, D.; Furche, F. *J. Chem. Phys.* **2010**, *133*, 134105.
(127) Valiev, M.; Bylaska, E. J.; Govind, N.; Kowalski, K.; Straatsma, T. P.; Van Dam, H. J. J.; Wang, D.; Nieplocha, J.; Apra, E.; Windus, T. L.; De Jong, W. a *Comput. Phys. Commun.* **2010**, *181*, 1477−1489.
(128) Pettersen, E. F.; Goddard, T. D.; Huang, C. C.; Couch, G. S.; Greenblatt, D. M.; Meng, E. C.; Ferrin, T. E. *J. Comput. Chem.* **2004**, *25*, 1605−12.
(129) Williams, T.; Kelley, C., et al. *Gnuplot 4.4: An interactive plotting program*, 2011. See also: http://www.gnuplot.info/.
(130) Gilson, M. K.; Irikura, K. K. *J. Phys. Chem. B* **2010**, *114*, 16304−16317.
(131) Goerigk, L.; Grimme, S. *Phys. Chem. Chem. Phys.* **2011**, *13*, 6670−6688.
(132) Fogueri, U. R.; Kozuch, S.; Karton, A.; Martin, J. M. L. *J. Phys. Chem. A* **2013**, *117*, 2269−2277.
(133) Goerigk, L.; Kruse, H.; Grimme, S. *ChemPhysChem* **2011**, *12*, 3421−3433.
(134) Liu, J.; Kelly, C. P.; Goren, A. C.; Marenich, A. V.; Cramer, C. J.; Truhlar, D. G.; Zhan, C.-G. *J. Chem. Theory Comput.* **2010**, *6*, 1109−1117.
(135) Ruzsinszky, A.; Perdew, J. P.; Tao, J.; Csonka, G. I.; Pitarke, J. M. *Phys. Rev. Lett.* **2012**, *109*, 233203.
(136) Perdew, J. P.; Ruzsinszky, A.; Sun, J.; Glindmeyer, S.; Csonka, G. I. *Phys. Rev. A* **2012**, *86*, 062714.
(137) Antony, J.; Brüske, B.; Grimme, S. *Phys. Chem. Chem. Phys.* **2009**, *11*, 8440−8447.
(138) Jurečka, P.; Šponer, J.; Černy, J.; Hobza, P. *Phys. Chem. Chem. Phys.* **2006**, *8*, 1985−93.
(139) Řezáč, J.; Riley, K. E.; Hobza, P. *J. Chem. Theory Comput.* **2011**, *7*, 2427−2438.
(140) Li, A.; Muddana, H. S.; Gilson, M. K. *J. Chem. Theory Comput.* **2014**, *10*, 1563−1575.
(141) Hostaš, J.; Řezáč, J.; Hobza, P. *Chem. Phys. Lett.* **2013**, *568*−*569*, 161−166.
(142) Li, A.; Muddana, H. S.; Gilson, M. K. *J. Chem. Theory Comput.* **2014**, *10*, 1563−1575.
(143) Witte, J.; Goldey, M.; Neaton, J. B.; Head-Gordon, M. *J. Chem. Theory Comput.* **2015**, *11*, 150317130807007.
(144) Grimme, S.; Steinmetz, M. *Phys. Chem. Chem. Phys.* **2013**, *15*, 16031−16042.
(145) Goerigk, L.; Reimers, J. R. *J. Chem. Theory Comput.* **2013**, *9*, 3240−3251.

DOI: 10.1021/acs.jctc.5b00296
J. Chem. Theory Comput. 2015, 11, 3785−3801